

**UNIVERSITY OF GAZİANTEP
GRADUATE SCHOOL OF
NATURAL & APPLIED SCIENCES**

**DETERMINATION OF TRAPPING
PARAMETERS FROM
THERMOLUMINESCENCE GLOW
CURVES BY COMPUTER GLOW
CURVE DECONVOLUTION METHOD**

**M. Sc. THESIS
IN
ENGINEERING PHYSICS**

**BY
ZAFER İNCE
JUNE 2011**

**GAZIANTEP ÜNİVERSİTESİ
FEN BİLİMLERİ ENSTİTÜSÜ**

**BİLGİSAYAR IŞILDAMA EĞRİSİ
AYRIŞIM METODU İLE
TERMOLÜMINESANS IŞILDAMA
EĞRİLERİNDEN TUZAK
PARAMETRELERİNİN
HESAPLANMASI**

**FİZİK MÜHENDİSLİĞİ
YÜKSEK LİSANS TEZİ**

**ZAFER İNCE
HAZİRAN 2011**

**Determination Of Trapping Parameters From
Thermoluminescence Glow Curves By Computer
Glow Curve Deconvolution Method**

**M.Sc. Thesis
in
Engineering Physics
University of Gaziantep**

**Supervisor
Prof. Dr. A. Necmeddin Yazıcı**

**by
Zafer İNCE
June 2011**

**Bilgisayar Işıldama Eğrisi Ayrışım Metodu İle
Termolüminesans Işıldama Eğrilerinden Tuzak
Parametrelerinin Hesaplanması**

**Gaziantep Üniversitesi
Fizik Mühendisliği
M.Sc. Tezi**

**Danışman
Prof. Dr. A. Necmeddin YAZICI**

**Zafer İNCE
Haziran 2011**

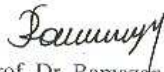
T.C.
UNIVERSITY OF GAZIANTEP
GRADUATE SCHOOL OF
NATURAL & APPLIED SCIENCES
DEPARTMENT OF ENGINEERING PHYSICS

Name of the thesis :Determination of Trapping Parameters from
Thermoluminescence Glow Curves by Computer Glow Curve
Deconvolution Method


Name of the student : Zafer Ince

Exam date : 08.06.2011


Approval of the Graduate School of Natural and Applied Sciences


Prof. Dr. Ramazan KOÇ

I certify that this thesis satisfies all the requirements as a thesis for the degree of
Master of Science/Doctor of Philosophy.


Prof. Dr. A. Necmeddin YAZICI
Head of Department

This is to certify that we have read this thesis and that in our consensus/majority
opinion it is fully adequate, in scope and quality, as a thesis for the degree of Master
of Science


Prof. Dr. A. Necmeddin YAZICI
Supervisor

Examining Committee Members




Title and Name-surname

Prof. Dr. A. Necmeddin YAZICI

Assoc. Prof. Dr. Mustafa ÖZTAS

Assoc. Prof. Dr. Metin BEDİR

.....

Signature




ABSTRACT

DETERMINATION OF TRAPPING PARAMETERS FROM THERMOLUMINESCENCE GLOW CURVES BY COMPUTER GLOW CURVE DECONVOLUTION METHOD

Zafer İNCE

M.Sc. in Engineering Physics

Supervisor: Prof.Dr.A.Necmeddin YAZICI

June 2011, 81 pages

In the given study, the synthetic glow curves were numerically obtained by directly solving the differential equations of thermoluminescence (TL) process without the use of approximating functions that have no physical meaning after different heating rates. The synthetic glow curves include a single TL glow peak. All of the simulated glow curves were analyzed by a glow curve deconvolution (fitting) program. The results of curve fitting program were compared with the input values to obtaining whether it reflects correct values of them or not. It was observed that the agreements between input parameters and results of curve fitting program are very good when the input parameters were chosen as very close to the first-order ($A_n \ll A_h$) and second-order ($A_n \approx A_h$) kinetics. Especially, if the concentration of trapped electrons (n_o) is equal or very close to the number of electron traps (N_t), the agreement between simulated and fitted glow curves becomes excellent. On the other hand, if the transition coefficient for electrons in the conduction band becoming trapped (A_n) is greater than the recombination transition coefficient for electrons in the conduction band with holes in centers (A_h), the agreement between numerically simulated and fitted glow curves is decreased. Especially, the success of fit is very bad at the high values of A_n/A_h ratios. As a result, the comparisons of resulting fitting parameters and input parameters indicate that the goodness of fit and agreement between input and fitted parameters are highly depend upon the ratio of transition coefficients (A_n/A_h) and occupancies of electron traps (n_o/N_t).

Keywords:

Thermoluminescence, computer glow curve deconvolution, curve fitting, numerical solutions, trapping parameters.

ÖZET

BİLGİSAYAR IŞILDAMA EĞRİSİ AYRIŞIM METODU İLE TERMOLÜMINESANS IŞILDAMA EĞRİLERİNDEN TUZAK PARAMETRELERİNİN HESAPLANMASI

Zafer İNCE

Yüksek Lisans Tezi, Fizik Mühendisliği Bölümü

Tez Yöneticisi: Prof.Dr.A.Necmeddin YAZICI

Haziran 2011, 81 sayfa

Bu yüksek lisans tezinde farklı ısıtma hızı oranlarında herhangi bir anlamı olmayan yaklaşım fonksiyonları kullanmaksızın termolüminesans diferansiyel denklemleri nümerik olarak çözümlenerek sentetik ışıldama eğrileri elde edildi. Elde edilen sentetik ışıldama eğrileri sadece bir ışıldama tepesi içermektedir. Tüm sentetik ışıldama eğrileri bilgisayar ile ışıldama eğrisi ayrışma metodu (eğri uydurma metodu) kullanılarak analiz edildi. Eğri uydurma metodunun sonucu, nümerik çözümlerde kullanılan giriş verileri ile karşılaştırılarak, doğru sonuç verip vermediği karşılaştırıldı. Eğri uydurma metodunun sonuçlarının giriş değerleri birinci dereceden ($A_n \ll A_h$) ve ikinci dereceden ($A_n \approx A_h$) TL kinetik denklemlerine yakın seçildiğinde aralarındaki uyumun oldukça güzel olduğu görüldü. Özellikle, elektron tuzakları tümüyle elektronlar tarafından doldurulduğunda ($n_o \approx N_t$), giriş değerleri ile eğri uydurma metodunun sonuçları mükemmel derecede uyum içinde olduğu görüldü. Diğer yandan, iletkenlik bandındaki elektronların yeniden elektron tuzaklarına geçiş katsayısı A_n 'nin, birleşme merkezlerine geçiş katsayısı A_h 'dan büyük olduğunda bu uyumun bozulmaya başladığı ve özellikle yüksek A_n/A_h oranlarında uyumun oldukça kötü olduğu görülmüştür. Sonuçta, eğri uydurma metodunun sonuçları ile giriş değerleri karşılaştırıldığında, aralarındaki uyumun elektron geçiş katsayılarının oranına (A_n/A_h) ile elektron tuzaklarındaki elektron konsantrasyonuna (n_o/N_t) oldukça bağlı olduğu elde edildi.

Anahtar Kelimeler:

Termolüminesans, bilgisayar ile ışıldama eğrisi ayrışım metodu, eğri uydurma, nümerik çözüm, tuzak parametreleri.

ACKNOWLEDGEMENT

I would like to express my gratitude to all those who gave me the possibility to complete this thesis.

I am deeply indebted to my supervisor Prof. Dr. A.Necmeddin YAZICI for whose helps, stimulating suggestions and encouragement helped me in all the time of research for and writing of this thesis. I want to thank them for all their helps, support, interest and valuable hints.

TABLE OF CONTENTS

ABSTRACT	2
ÖZET	3
ACKNOWLEDGEMENT	4
TABLE OF CONTENTS	5
LIST OF TABLES	6
LIST OF FIGURES	7
LIST OF SYMBOLS	9
CHAPTER 1	11
INTRODUCTION	11
CHAPTER 2	13
THEORY OF THERMOLUMINESCENCE	13
2.1 Luminescence	13
2.3 Basic concepts of thermoluminescence	16
2.4 The One Trap–One Centre Model	20
2.5 Trap-Filling Process	21
2.6 Trap-Emptying Process	22
2.7 First-order kinetics	25
2.8 Second-order kinetics	28
2.9 General-order kinetics	30
2.10 Advanced models	31
2.11 Trapping Parameters Determination Methods	33
2.12 CGCD Method	34
2.13 Mathematica	36
CHAPTER 3	40
NUMERICAL CALCULATIONS AND RESULTS	40
CONCLUSION	70
REFERENCES	73

LIST OF TABLES

Table 1: The below table includes some of the input parameters which were used in numerical simulated TL glow curves and obtained kinetic parameters after their analyzing by curve fitting program.....	55
Table 2: The below table includes some of the input parameters which were used in numerical simulated TL glow curves and obtained kinetic parameters after their analyzing by curve fitting program.....	56
Table 3: The below table includes some of the input parameters which were used in numerical simulated TL glow curves and obtained kinetic parameters after their analyzing by curve fitting program.....	57
Table 4: The below table includes some of the input parameters which were used in numerical simulated TL glow curves and obtained kinetic parameters after their analyzing by curve fitting program.....	58
Table 5: The below table includes some of the input parameters which were used in numerical simulated TL glow curves and obtained kinetic parameters after their analyzing by curve fitting program.....	59

LIST OF FIGURES

Figure 1: Common electronic transitions in crystalline solids: (1) ionization; (2) and (3) electron and hole trapping respectively; (4) and (5) electron and hole release; (6) direct recombination; (7), (8), (9), (10) indirect recombination. (ET: Electron Trap; HT=Hole Trap; R_1 , R_2 , and R_3 Recombination Centers) [6]. 15

Figure 2: Phenomena of thermal excitation of luminescence. 17

Figure 3: Simple diagram of a TL reader system with heater plate, photomultiplier detector and readout electronics [6]. 18

Figure 4: An analyzed glow curve of 1% Al-doped LiB_3O_5 obtained at a heating rate of $1^\circ\text{C}/\text{sec}$ following β -ray exposure at room temperature for 5 min (≈ 4.5 Gy) (The open circles represent the experimental points, the full curve is the global fitting and broken curves represent fitted individual glow peaks.) [13]. 19

Figure 5: Simple band model for TL emission. Allowed transitions: (1) thermal release, (2) migration in the conduction band, (3) radiative recombination. 21

Figure 6: Properties of the Randall–Wilkins first-order TL equation, showing: (a) variation with n_0 , the concentration of trapped charge carriers after irradiation; (b) the variation with E , the activation energy; (c) the variation with s , the escape frequency; (d) the variation with β , the heating rate. Parameter values: $n_0=1\text{ m}^{-3}$; $E=1\text{ eV}$; $s=1\times 10^{12}\text{ s}^{-1}$, $\beta=1\text{ K/s}$ of which one parameter is varied while the others are kept constant [16]. 27

Figure 7: Properties of the Garlick–Gibson second-order TL equation, showing: (a) variation with n_0 , the concentration of trapped charge carriers after irradiation; (b) the variation with E , the activation energy; (c) the variation with s/N ; (d) the variation with β , the heating rate. Parameter values: $n_0=1\text{ m}^{-3}$; $E=1\text{ eV}$; $s/N=1\times 10^{12}\text{ s}^{-1}\text{ m}^3$, $\beta=1\text{ K/s}$ of which one parameter is varied while the others are kept constant [16]. 30

Figure 8: Comparison of first-order ($b=1$), second-order ($b=2$) and intermediate-order ($b=1.3$ and 1.6) TL peaks, with $E=1\text{ eV}$, $s=1\times 10^{12}\text{ s}^{-1}$, $n_0=N=1\text{ m}^{-3}$ and $\beta=1\text{ K/s}$ [3]. 31

Figure 9: Advanced models describing the thermally stimulated release of trapped charged carriers including: (a) a shallow trap (ST), a deep electron trap (DET), and a active trap (AT); (b) two active traps and two recombination centers; (c) localized transitions; (d) defect interaction (trapping centre interacts with another defect) [3]. 33

Figure 10: The numerically simulated (open circles) and fitted (red solid line) glow curves of $\sin 3$, $\sin 9$, $\sin 15$ and $\sin 20$ 60

Figure 11: The numerically simulated (open circles) and fitted (red solid line) glow curves of $\sin 27$, $\sin 34$, $\sin 40$ and $\sin 42$ 61

Figure 12: The numerically simulated (open circles) and fitted (red solid line) glow curves of $\sin 43$, $\sin 50$, $\sin 54$ and $\sin 57$ 62

Figure 13: The numerically simulated (open circles) and fitted (red solid line) glow curves of sin66, sin71, sin72 and sin73.	63
Figure 14: The numerically simulated (open circles) and fitted (red solid line) glow curves of sin77, sin84, sin91 and sin97.	64
Figure 15: The numerically simulated (open circles) and fitted (red solid line) glow curves of sin104, sin111, sin116 and sin122.....	65
Figure 16: The numerically simulated (open circles) and fitted (red solid line) glow curves of sin129, sin135, sin141 and sin145.....	66
Figure 17: The numerically simulated (open circles) and fitted (red solid line) glow curves of sin151, sin157, sin165 and sin169.....	67
Figure 18: The numerically simulated (open circles) and fitted (red solid line) glow curves of sin174, sin178, sin181 and sin187.....	68
Figure 19: The numerically simulated (open circles) and fitted (red solid line) glow curves of sin191, sin195 and sin198.....	69

LIST OF SYMBOLS

A	: Integrated area of the fitted glow curve
a	: Electronic noise contribution to the planchet
A_h	: Recombination transition coefficient for electrons in the conduction band with holes in centers
A_n	: Transition coefficient for electrons in the conduction band becoming trapped (volume/until time $\text{m}^3\text{sec}^{-1}$)
A_m	: Transition coefficient for holes in the valance band becoming trapped in the hole centers
AT	: Active Trap
α	: alpha rays
b	: Kinetic order
β	: Heating rate
β	: beta rays
CB	: Conduction Band
CGCD	: Computer Glow Curve Deconvolution
DET	: Deep Electron Trap
E or E_a	: Activation energy (trap depth)
E_c	: Bottom of the conduction band
E_f	: Energy Fermi level
E_g	: Band gap
E_v	: Top of the valance band
ET	: Electron Traps
f	: Electron-hole generation rate
FOM	: Figure of Merit
HT	: Hole Traps
I	: Thermoluminescence intensity
I_m	: Peak intensity
k	: Boltzman's Constant
N	: Concentration of available electron traps in the crystal (in m^{-3}),
n	: Concentration of the filled electron traps in the crystal (in m^{-3})
n_o	: Number of trapped electrons at the initial time $t_0 = 0$
n_c	: Concentration of electrons in the conduction band (per unit volume m^{-3})
N_h	: Concentration of available hole centers,
n_h	: Concentration of holes in the recombination centers
N_i	: i -th experimental points
n_v	: Concentration of holes in the valance band
m	: Concentration of holes trapped at R (m^{-3})
OSL	: Optically Stimulated Luminescence
p	: Probability per unit time of release of an electron from the trap
R	: Recombination centers
s	: frequency factor
ST	: Shallow Trap
T	: Temperature

T_0 : Room temperature
 T_m : Peak temperature
 γ : Gamma rays
 t : Time
 τ : Life time
TL : Thermoluminescence
TLD : Thermoluminescence Dosimetry
TSC : Thermally Stimulated Luminescence
UV : Ultraviolet
VB : Valance Band

CHAPTER 1

INTRODUCTION

When an insulating crystal is exposed to ionizing radiation, free electrons and holes are produced. Then, some of these holes and electrons are trapped in defects in the crystal lattices of the solid. Subsequently, if the temperature is raised to a high temperature enough to cause the removal of electrons from their traps, they wander around until they recombine with holes at recombination centers giving off light. This phenomenon is called as thermoluminescence (TL). The curve plotted versus temperature is called as thermoluminescence (TL) glow curve. The shape and position of the resultant TL glow curves can be analyzed to extract information on the various kinetic parameters of the trapping process; trap depth, frequency factor, trapping and retrapping rates, kinetic order and etc. The physical mechanisms governing the trapping and release of electrons are discussed in detail in the text by McKeever [1]. The rate equations describing these physical processes at a single type of trap (one trap one recombination center (OTOR)) can be solved under various assumptions, and analytical expressions are obtained for the shape of the resulting glow curve. Experimentally observed glow curves are analyzed by fitting them to the analytical expressions by computer glow curve deconvolution (CGCD) program [2], and the kinetic parameters are determined from the fitting process [3-5]. The application of this method for the decomposition of a composite thermoluminescence glow-curve into its individual glow-peaks is widely applied since 1980 [2]. This method has become very popular method to obtain kinetic (trapping) parameters for the last two decades and it has great advantages over the other experimental methods (i.e. initial rise, peak shape, heating rate and etc) owing to simultaneous determination of trapping parameters of all glow peaks without additional thermal treatments and experimental repetitions.

The purpose of the present study is to investigate how well this fitting process (computer glow curve deconvolution process) works in providing reliable values for

the kinetic parameters of the traps. The relevant rate equations describing the flow of electrons between traps and the luminescence center were used without approximation to numerically generate simulated TL glow curves for a wide range of trapping parameters. The simulated glow curves were analyzed by the usual method of fitting them to one of the analytical expressions, and the kinetic parameter values determined by this fitting procedure were compared with the values used in generating the glow curves. We were comment on the comparisons, and endeavor to derive some useful insights to assist in the interpretation and analysis of experimentally measured TL glow curves.

CHAPTER 2

THEORY OF THERMOLUMINESCENCE

2.1 Luminescence

Luminescence is a light phenomenon which is observed when an irradiated insulator or wide band-gap semiconductor is stimulated by excitation energy. This excitation energy classifies the luminescence. The different kinds of luminescence phenomena are defined according of the simulation method causing light emission. The most known of luminescence are:

- Thermoluminescence : released by increasing temperature;
- Photoluminescence : obtained by stimulation with UV light;
- Radioluminescence : stimulated by ionizing radiation;
- Triboluminescence : stimulation due to mechanical stress;
- Chemiluminescence : stimulated by chemical reactions;
- Phosphorescence : excited by ionizing radiation, UV and visible light.

The process of emission by thermal stimulation from a crystalline solid after irradiations is called as “thermally stimulated process or simply” thermoluminescence (TL) [1]. The TL belongs the class of phenomena involving light emission from solids (insulators or semiconductors) and then labeled as luminescence. The storage of radiation energy is an important feature for dosimetry which is generally favored by presence of activators namely impurity atoms and structural defects.

When we characterize atoms of a crystal by three-dimensional periodicity it is observed that there are some point defects within the crystal. A real crystal may contain defects which are basically of the following types;

1. Intrinsic defects; vacancies (or missing atoms), interstitials, aggregate forms of previous defects.
2. Defects induced by ionizing radiations: F centers, V centers, V_k centers, etc.
3. Extrinsic (or impurity) defects: substitutional impurities, interstitial impurities.

The property of storing energy is due to the presence of crystal defects such as vacancies and impurities. The luminescence phenomena can be observed due to all defects can be potentially acted as traps or recombination center for charge carriers created by suitable excitation. The defects are able to capture the electrons and holes generated in the irradiation process. A crystal defect is classified as a trap center if the defect is able to capture a charge carrier and reemit it back to the band it come from. A crystal defect where carriers of opposite sign can be captured, resulting in an electron-hole recombination, is classified as a recombination center. Efficient thermoluminescent materials have a high concentration of traps and recombination centers, provided by structural defects and impurities [6].

2.2 Band Model and Electronic Transitions in Insulators and Semiconductors

The band model of an insulator or semiconductor can be described quantum mechanically and the energy band theory of solids explains the observed TL properties [3]. In an ideal semiconductor or insulator crystalline most of the electrons reside in the valence band. The next highest band that the electrons can occupy is the conduction band, separated from the valence band by the so-called forbidden band gap. The energy difference between the valence band and conduction band is E_g . Figure 1 shows schematically the energy band models of an insulator, the electronic energy levels within the forbidden energy gap, and the common electronic transitions in these levels [6].

For a crystal without lattice defects there are no energy levels between the valence and conduction bands. The energy levels introduced may be discrete, or may be distributed depending upon the exact nature of the defect and of the host lattice. In general terms, it is believed that the lattice imperfections, impurities, intrinsic and extrinsic defects give rise to the localized energy levels (metastable state) within the forbidden energy gap. A free electron in these crystals may become attracted by columbic field of a vacant anion site and become trapped. The energy required to release the electron from the trap is less than that required to free a valence electron and thus anion vacancy has associated with it an energy level which lies somewhere between the valence and the conduction bands. A similar situation is satisfied for hole which is trapped with cation vacancies and once again they give localized energy levels within the band gap. Similar arguments apply to the incorporation of impurity ions

(cation or anion) within the crystal lattice, either in substitutional or interstitial positions. Thus, localized energy levels can act either as traps or as recombination centers. The defect where the electron is released is called trapping center or trap. The defect where the electron and hole recombine is called recombination center or luminescent center if this recombination produces a photon. In principle it is believed that recombination centers are located towards the middle of the forbidden gap and traps are located towards the edges of corresponding bands. However, a center becomes trap at high temperatures, but may become recombination center at low temperatures [6].

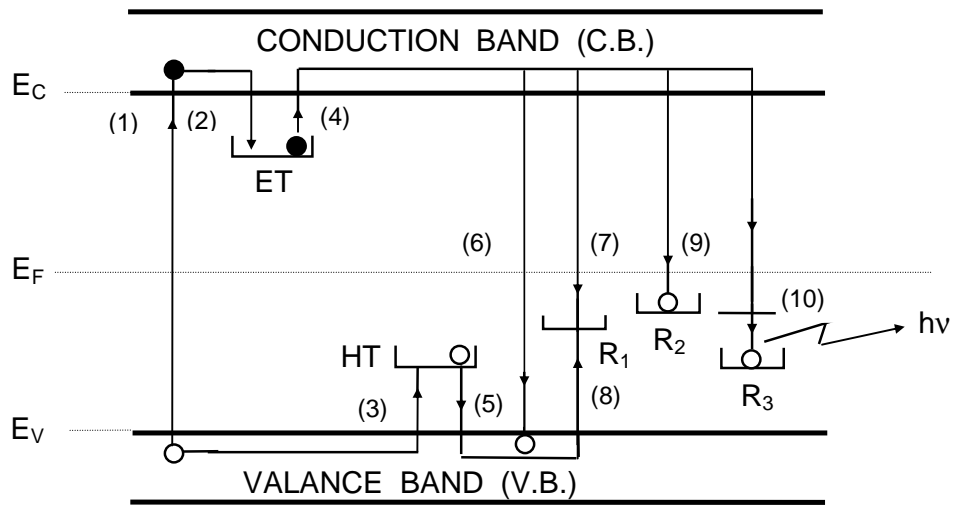


Figure 1. Common electronic transitions in crystalline solids: (1) ionization; (2) and (3) electron and hole trapping respectively; (4) and (5) electron and hole release; (6) direct recombination; (7), (8), (9), (10) indirect recombination. (ET: Electron Trap; HT=Hole Trap; R_1 , R_2 , and R_3 Recombination Centers) [6].

During the irradiations of crystals with $h\nu > E_g$ (i.e. by UV lights, α , β and γ -radiations) correspond to the liberation of an electron from the valence band into the conduction band leaving a hole in the valence band (transition (1)). Thus, transition (1) corresponds to the process of ionization. The free electron in the conduction band and free hole in the valence band wander through the crystal until they become trapped at the lattice defects. The electron may be trapped by a transition to the lowest available energy level at the defect (transition (2)). The hole may be also be trapped at a lattice defect above the valence band (transition (3)). The trapped electrons and holes may be released from the traps when the crystal is heated or under the optical excitation (transition (4) and (5)) [6].

The probability of a charge carrier being thermally released from its trap is exponentially related to $-E/kT$, where E is called as "trap depth" which is the energy difference between the trap and conduction band (for electrons) or the valance band (for holes), T is the temperature at which charge carriers are being excited from their corresponding delocalized band.

When the charge carriers are released to their corresponding band, they are once again free to move through the crystal and may recombine with a charge carrier of opposite sign, either directly (transition (6)), or indirectly (transitions (7), (8) and (9)). The band-to-band recombination may be termed as "direct", whilst recombination involving localized levels, i.e. band to center or center-to-center, may be termed as "indirect". If either of these recombination mechanisms is accompanied by the emission of light then luminescence results (radiative transitions). When the free electron transits to an excited state from conduction band due to the relaxation of the lattice around the defect according to new situation, no photon is emitted (non-radiative transitions). But the new situation is not stable, the excited electron transits to the ground state via emitting a photon (transition (10)).

By heating the crystal captured electrons and holes can be freed thermally into the conduction or valance band and then make a transition to the radiative recombination center R. This process is termed thermally stimulated luminescence (TL). Alternatively, external light exposure of the crystal can release captured electrons from a trap center to the conduction band from where they can recombine into the recombination center R. This phenomenon is termed optically stimulated luminescence (OSL) [3]. The optically or thermally freed charge carriers in the conduction/valance band can be measured as electrical current when applying voltage across the crystal. These measurements are termed thermally and optically stimulated conductivity (TSC, OSC), respectively [3].

2.3 Basic concepts of thermoluminescence

The phenomenon thermoluminescence has been known for a long time. The first application of this phenomenon for dosimetric purposes was from Daniel et al. [7]. Since then much research has been carried out for a better understanding and improvement of the material characteristics as well as to develop new TL materials. Nowadays, thermoluminescence dosimetry (TLD) is a well-established dosimetric

technique with applications in areas such as personnel, environmental and clinical dosimetry [8-12].

Thermoluminescence (TL) is the physical phenomenon in which a solid sample absorbs energy while irradiated at a given temperature, and releases this energy in the form of light while heating the sample. TL should not be confused with the light spontaneously emitted from a substance when it is heated to incandescence. At higher temperatures (say in excess of 200°C) a solid emits (infra) red radiation of which the intensity increases with increasing temperature. This is thermal or black body radiation. TL, however, is the thermally stimulated emission of light following the previous absorption of energy from radiation. According to this phenomenon, the three essential ingredients necessary for the production of TL can be deduced. Firstly, the material must be an insulator or semiconductor—metals do not exhibit luminescent properties.

Secondly, the material must have at some time absorbed energy during exposure to ionizing radiation. Thirdly, the luminescence emission is triggered by heating the material [1]. A thermoluminescent material is a material that absorbs some energy which is stored during exposure to ionizing radiation. When the material is heated, the stored energy is released in the form of visible light as seen in Fig.2. In fact that TL does not refer to thermal *excitation*, but to *stimulation* of luminescence in a sample which was excited in a different way. TL material can not emit light again by simply cooling the sample and reheating it another time. It should first be re-exposed to ionizing radiation before it produces light again. The storage capacity of a TL material makes it suitable for dosimetric applications.

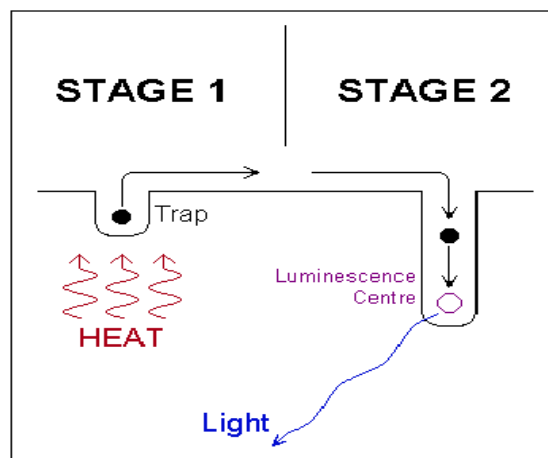


Figure 2. Phenomena of thermal excitation of luminescence.

A simplified set up diagram for measuring TL is shown in Fig.3 and a typical TL glow curve obtained from an Al-doped LiB_3O_5 sample is shown in Fig.4. The emitted light is recorded as intensity vs. temperature in the shape of one or more TL peaks. Although a TL glow curve may look like a smooth continuum, it is composed of a number of overlapping peaks derived from the thermal release of electrons from traps of different stabilities. The lifetime of electrons in deep traps is longer than that of electrons in shallow traps. Under favorable conditions, the emitted TL light intensity is proportional to the absorbed dose, and thus, using an appropriate calibration, one can evaluate the applied dose in the given radiation field. The TL signal may be the intensity at the maximum or the area under the TL glow peak, which are usually nearly proportional to each other. In “regular” dosimetric applications, one can choose an appropriate material with reproducible results in repeated measurements, linear dose dependence for the kind of radiation in question as well as dose-rate independence and long time stability.

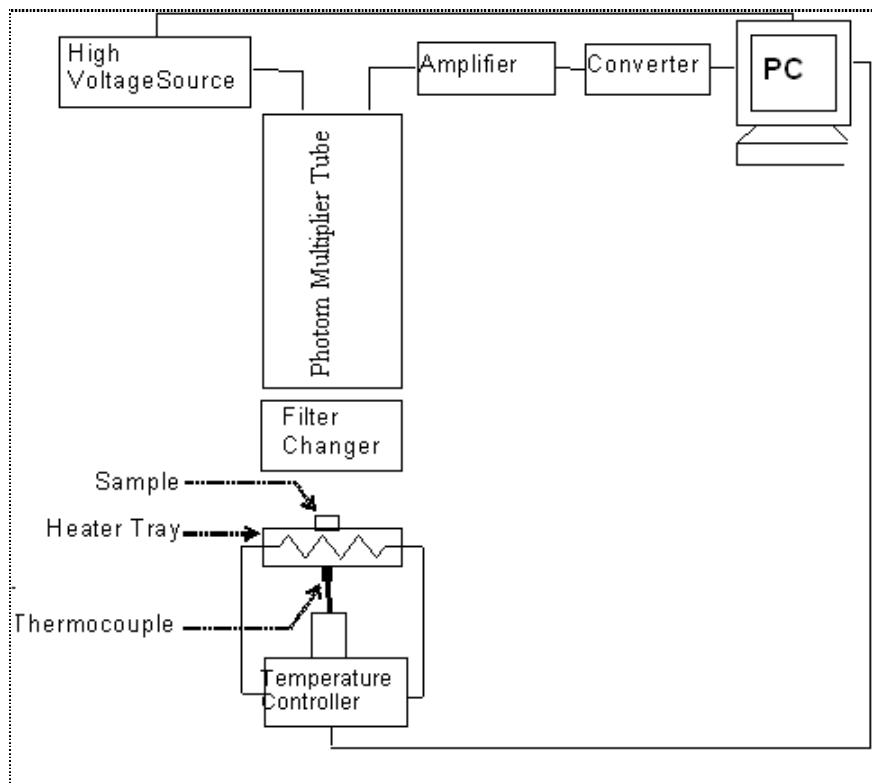


Figure 3. Simple diagram of a TL reader system with heater plate, photomultiplier detector and readout electronics [6].

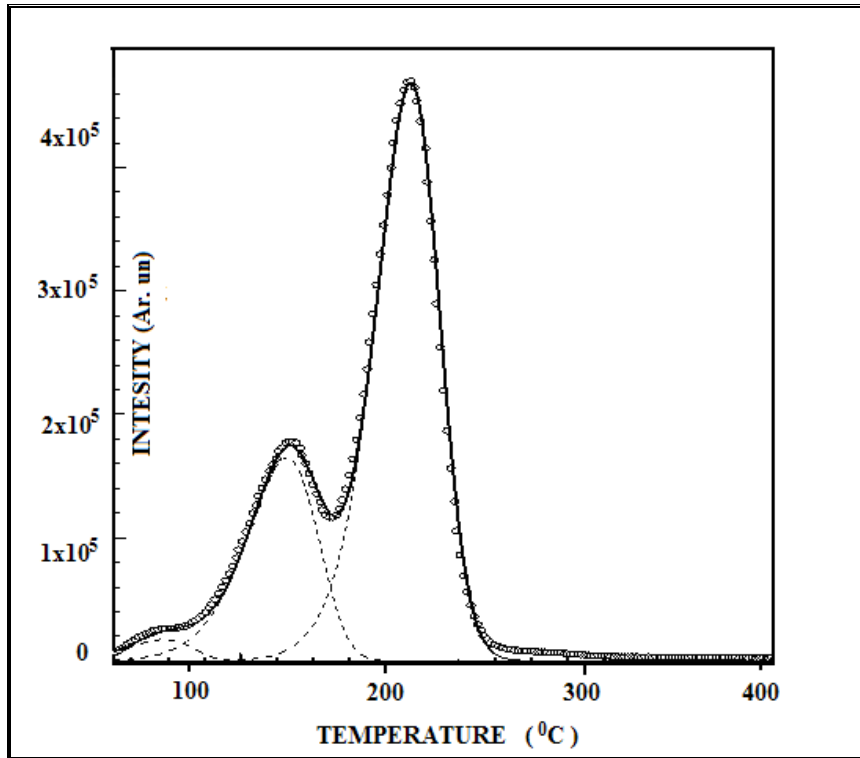


Figure 4. An analyzed glow curve of 1% Al-doped LiB_3O_5 obtained at a heating rate of $1^\circ\text{C}/\text{sec}$ following β -ray exposure at room temperature for 5 min (≈ 4.5 Gy) (The open circles represent the experimental points, the full curve is the global fitting and broken curves represent fitted individual glow peaks.) [13].

The aim of a mathematical analysis concerning the thermoluminescent emission of light is to achieve a satisfactory knowledge of the phenomena related to it. From a theoretical point of view, TL is directly connected to the band structure of solids and particularly to the effects of impurities and lattice irregularities. The mapping of the forbidden gap reveals quite a complex configuration, and the experimental TL emission study can provide a satisfactory tool to get detailed information on its most meaningful parameters. These are, for each site, the characteristic activation energy (E), a frequency factor (s), connected to the transition frequency, and a kinetic order (b) synthesizing the quality of the involved phenomena [1].

The kinetic order ranges between 1 and 2. The former value corresponds to a situation where a charge (electron) is supplied energy to raise in the conduction band and, consequently, to fall to a center where it undergoes recombination with hole; the latter one stands for a situation where this phenomenon has the same probability of retrapping. Intermediate cases are likely to occur as well as contributions from non-radiative events ($b = 0$). The mathematical models based upon these definitions are

consisting of convenient differential equations systems, yielding for each case, the evolution of charged carrier populations, the analytical forms of which are to be checked by means of suitable experimental data. It is therefore evident how the involved parameters are to be conveniently adjusted until a fair agreement between theory and practice is attained. The most promising tool is the observation and the recording of TL emission, under several experimental conditions, as a function of temperature which the TL sample is heated to, or of heating up time. For a constant heating rate, these two observations are equivalent. The plot shape depends on the physical and chemical properties of the material and on the kind of the treatment it is submitted to. However it is always a single- or multi-peaks structure, as may be expected from the general equations, and a correspondence can be pointed out between a peak and an electron trap level. This is explained by considering how, at a certain temperature, the amount of thermal energy supplied reaches, for a given level, the threshold necessary to raise the relative trapped charges in the conduction band from where they can give rise to radiative recombination events. For this purpose, other centers, able to trap positive charge carriers, are involved, and they are likely to be connected to the quality of the emitted light. The analytical form for a single peak, which the overall curve is a superposition of, can fully described by means of some geometrical parameters as the peak position, its left and right widths, the ratio between them, the overall width, the height. This last one is dependent on the heating rate and increases, for given experimental conditions, with the increasing of it. These geometrical parameters can be shown to correspond to the main physical ones: the mathematical expressions can be evaluated by a convenient analytical manipulation of the involved equations. It is also to be remarked that the experimental uncertainties, obtained by means of the glow-curve plot, allow for an estimate of the physical errors related to them, and their evaluations can point out a well defined method as the fittest one.

2.4 The One Trap–One Centre Model

The simplest model for TL consists of a single type of electron defect level (electron traps-T) and a single type of hole defect level (recombination center-R) in the forbidden gap, as depicted in Figure 5 [3]. It must be required to remember in here that

two energy level band model is the minimum number needed in order to describe the thermoluminescence mechanism. But, the band model of an actual specimen may be much more complex than this simple model. However, this simple model is enough to explain the fundamental features of TL production.

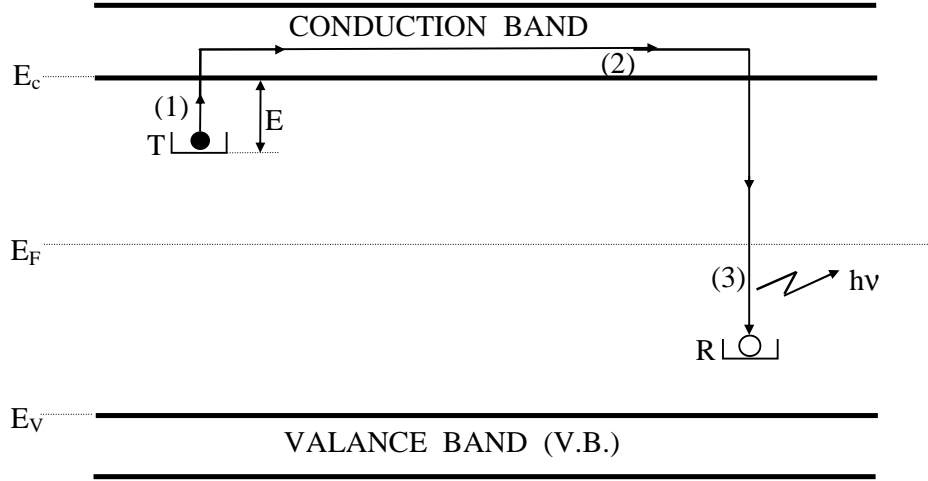


Figure 5. Simple band model for TL emission. Allowed transitions: (1) thermal release, (2) migration in the conduction band, (3) radiative recombination.

2.5 Trap-Filling Process

During the irradiation, the differential equations governing the traffic of electrons between the trap level, the recombination center and the conduction band are [1,3]:

$$\frac{dn_c}{dt} = f - n_c n_h A_h - n_c (N - n) A_n \quad (1)$$

$$\frac{dn}{dt} = n_c (N - n) A_n \quad (2)$$

$$\frac{dn_v}{dt} = f - n_v (N_h - n_h) A_m \quad (3)$$

$$\frac{dn_h}{dt} = n_v (N_h - n_h) A_m - n_c n_h A_h \quad (4)$$

The meaning of variables used in this model (OTOR) is that: E =activation energy of the electron traps (in eV), s =frequency factor of the electron trap (in s^{-1}), n_c is the concentration of electrons in the conduction band (per unit volume m^{-3}), n_v is the concentration of holes in the valance band, N is the concentration of available electron traps (of depth E below the conduction band) in the crystal (in m^{-3}), n is the concentration of the filled electron traps in the crystal (in m^{-3}), n_h is the concentration of

holes in the recombination centers, N_h is the concentration of available hole centers, A_n is the transition coefficient for electrons in the conduction band becoming trapped (volume/unit time $\text{m}^3\text{sec}^{-1}$), A_m is the transition coefficient for holes in the valence band becoming trapped in the hole centers, A_h is recombination transition coefficient for electrons in the conduction band with holes in centers and f is the electron hole generation rate.

2.6 Trap-Emptying Process

If the trap depth $E \gg kT_0$, where k is Boltzmann's constant $= 8.617 \times 10^{-5}$ eV/K and T_0 is the irradiation temperature (i.e. room temperature), trapped electrons will remain for a long period of time in traps, until exposure to the radiation there will exist a substantial population of trapped electrons. There must be an equal population of trapped holes at level R, due to the free electrons and holes created and annihilated in pairs. Because the normal equilibrium Fermi level E_f is situated below level T and above level R, these populations of trapped electrons and holes represent a non-equilibrium state. The reaction path for return to equilibrium is always open and the probability (p) per unit time of release of an electron from the trap is assumed to be described by the Arrhenius equation,

$$p = s \exp\left\{-\frac{E}{kT}\right\} \quad (5)$$

The perturbation from equilibrium (during exposure to ionizing radiation) was performed at low temperature (compared to E/k), the relaxation rate as determined by above equation is slow. Thus, the non-equilibrium state is metastable and will exist for an indefinite period, governed by the rate parameters E and s . The life time, τ , of the charge carrier in the metastable state at temperature T , is given by

$$\tau = p^{-1} \quad (6)$$

If n is the number of trapped electrons in T , and if the temperature is kept constant, then n decreases with time t according to the following expression:

$$\frac{dn}{dt} = -np \quad (7)$$

Integrating this equation

$$\int_{n_0}^n \frac{dn}{n} = -\int_{t_0}^t p \cdot dt \quad (8)$$

one obtains

$$n = n_o \cdot \exp \left[-s \exp \left\{ -\frac{E}{kT} \right\} t \right] \quad (9)$$

where n_o is the number of trapped electrons at the initial time $t_0 = 0$. Assuming now the following assumptions:

- irradiation of the thermoluminescent material at a low enough temperature so that no electrons are released from the trap,
- the life time of the electrons in the conduction band is short,
- all the released charges from trap recombine in luminescent center,
- the luminescence efficiency of the recombination centers is temperature independent,
- the concentrations of traps and recombination centers are temperature independent,
- no electrons released from the trap is retrapped.

The return to equilibrium can be speeded up by raising the temperature of the TL material above T_0 . This will increase the probability of detrapping and the electrons will now be released from the trap into the conduction band. The charge carrier migrates through the conduction band of the crystal until it undergoes recombination at recombination centre R. In the simple model this recombination centre is a luminescent centre where the recombination of the electron and hole leaves the centre in one of the higher excited states. Return to the ground state is coupled with the emission of light quanta, i.e. TL. The intensity of TL in photons $I(t)$ per second at any time t during heating is proportional to the rate of recombination of holes and electrons at R. If m (m^{-3}) is the concentration of holes trapped at R the TL intensity can be written as

$$I(t) = -\frac{dm}{dt} \quad (10)$$

Here we assume that each recombination produces a photon and that all produced photons are detected. The rate of recombination will be proportional to the concentration of free electrons in the conduction band n_c and the concentration of holes m ,

$$I(t) = -\frac{dm}{dt} = n_c m A_h = n_c (n + n_v) A_h \quad (11)$$

with the constant A_h the recombination probability expressed in units of volume per unit time which is assumed to be independent of the temperature. The rate of change of the concentration of trapped electrons n is equal to the rate of thermal release minus the rate of retrapping,

$$-\frac{dn}{dt} = np - n_c(N - n)A_n = ns \exp\left\{-\frac{E}{kT}\right\} - n_c(N - n)A_n \quad (12)$$

with N the concentration of electron traps and A_n the probability of retrapping (m³/s). Likewise the rate concentration of free electrons is equal to the rate of thermal release minus the rate of retrapping and the rate of recombination,

$$\frac{dn_c}{dt} = ns \exp\left\{-\frac{E}{kT}\right\} - n_c(N - n)A_n - n_c mA_h \quad (13)$$

Equations (11-13) described the charge carrier traffic in the case of release of a trapped electron from a single-electron trap and recombination in a single centre. For TL produced by the release of holes the rate equations are similar to Eqn.(11-13). These equations form the basis of many analyses of TL phenomena. The equation (12) express mathematically the fact that electrons in the trap cab be either thermally excited in the conduction band ($ns \exp\{-E/kT\}$) or they can be retrapped in the trap with a probability coefficient $A_n(n_c(N - n))$. The equation (13) represents the change in the concentration of the electrons in the conduction band n_c . The concentration of these free electrons in the conduction band can be reduced by either trafficking into the trap ($-dn/dt$), or by recombination in the RC with a probability coefficient $A_n(-A_h n_c(n + n_c))$. The equation (11) describes the rate of change of the concentration of holes trapped in the RC and the right-hand side representing the rate of change of the total concentration of electrons in the crystal. Unfortunately, there is no general analytical solution of these equations. To develop an analytical expression some simplifying assumptions must be additionally made. An important assumption is at any time

$$\left|\frac{dn_c}{dt}\right| \ll \left|\frac{dn}{dt}\right|, \quad \left|\frac{dn_c}{dt}\right| \ll \left|\frac{dm}{dt}\right| \quad (14)$$

This assumption is called by Chen and McKeever [3] the quasi-equilibrium assumption since it requires that the free electron concentration in the conduction

band is quasi-stationary. The trapped electrons and holes are produced in pairs during the irradiation. Charge neutrality dictates therefore

$$n_c + n = m \quad (15)$$

which for $n_c \approx 0$ means that $n \approx m$ and

$$I(t) = -\frac{dm}{dt} \approx -\frac{dn}{dt} \quad (16)$$

Since $dn/dt \approx 0$ one gets from equation (11) and (12):

$$I(t) = \frac{mA_n n s \exp\left\{-\frac{E}{kT}\right\}}{(N-n)A_h + mA_n} \quad (17)$$

2.7 First-order kinetics

Even Eqn.(17) cannot be solved analytically without additional simplifying assumptions. Randall and Wilkins [14-15] assumed negligible retrapping during the heating stage, i.e. they assumed $mA_n \gg (N-n)A_h$. Under this assumption Eqn.(17) can be written

$$I(t) = -\frac{dn}{dt} = sn \exp\left\{-\frac{E}{kT}\right\} \quad (18)$$

This differential equation describes the charge transport in the lattice as a first-order process and the glow peaks calculated from this equation are called first-order glow peaks. Solving the differential Eqn.(18) yields

$$I(t) = -\frac{dn}{dt} = n_0 s \exp\left\{-\frac{E}{kT}\right\} \exp\left\{-s \int_0^t \exp\left\{-\frac{E}{kT(t')}\right\} dt'\right\} \quad (19)$$

where n_0 is the total number of trapped electrons at time $t=0$. Usually the temperature is raised as a linear function of time according to

$$T(t) = T_0 + \beta t \quad (20)$$

with β the constant heating rate and T_0 the temperature at $t=0$. With using eq.(20), heating rate can be written as $\beta=dT/dt$ and introducing it into equation (14)

$$\int_{n_0}^n \frac{dn}{n} = -\left(\frac{s}{\beta}\right) \int_{T_0}^T \exp\left(-\frac{E}{k.T'}\right) dT' \quad (21)$$

And the number of trapped electrons (n) in term of β

$$n = n_0 \cdot \exp\left[-\left(\frac{s}{\beta}\right) \int_{T_0}^T \exp\left(-\frac{E}{k.T'}\right) dT'\right] \quad (22)$$

This gives for the intensity as function of temperature

$$I(T) = -\frac{1}{\beta} \frac{dn}{dt} = n_0 \frac{s}{\beta} \exp\left\{-\frac{E}{kT}\right\} \exp\left\{-\frac{s}{\beta} \int_{T_0}^T \exp\left\{-\frac{E}{kT'}\right\} dT'\right\} \quad (23)$$

This is the well-known Randall–Wilkins first-order expression of a single glow peak. The peak has a characteristic asymmetric shape being wider on the low temperature side than on the high temperature side. On the low temperature side, i.e. in the initial rise of the glow peak, the intensity is dominated by the first exponential ($\exp(-E/kT)$). Thus, if I is plotted as function of $1/T$, a straight line is expected in the initial rise temperature range, with the slope of $-E/k$, from which the activation energy E is readily found.

The properties of the Randall–Wilkins equation are illustrated in Fig.6. In Fig.6(a) it is shown how $I(T)$ varies if n_0 varies from $n_0=0.25 \text{ m}^{-3}$ till $n_0=2 \text{ m}^{-3}$ while $E=1 \text{ eV}$, $s=1.0 \times 10^{12} \text{ s}^{-1}$ and $\beta=1 \text{ K/s}$ are kept constant. It can be noted that the temperature at the peak maximum, T_m , stays fixed. This is a characteristic of all first-order TL curves. The condition for the maximum can be found by setting $dI/dt=0$ (or, somewhat easier from $d \ln I(T)/dt=0$). From this condition one gets

$$\frac{\beta E}{kT_m^2} = s \exp\left\{-\frac{E}{kT_m}\right\} \quad (24)$$

In this equation n_0 does not appear which shows that T_m does not depend on n_0 . From Fig.6(a) it can be further seen that not only the peak height at the maximum but each point of the curve is proportional to n_0 . In the application in dosimetry n_0 is the parameter of paramount importance since this parameter is proportional to the absorbed dose. It is simple to see that the area under the glow peak is equal to n_0 since

$$\int_0^{\infty} I(t) dt = -\int_0^{\infty} \frac{dn}{dt} dt = -\int_{n_0}^{n_{\infty}} dn = n_0 - n_{\infty} \quad (25)$$

and n_{∞} is zero for $t \rightarrow \infty$. In Fig.6(b) the activation energy E has been varied from 0.8 to 1.2 eV. As E increases the peak shifts to higher temperatures with a decrease in the height and an increase in the width keeping the area (i.e. n_0) constant.

Similar changes can be noticed as s is varied (see Fig.6(c)) but now in the opposite way: as s increases the peak shifts to lower temperatures with an increase of the height and a decrease in width. In Fig.6(d) the heating rate has been varied. As β increases the peak shifts to higher temperatures while the height decreases and the

width increases just as in the case of decreasing s . This can be expected since s and β appear as a ratio s/β in Eqn.(23).

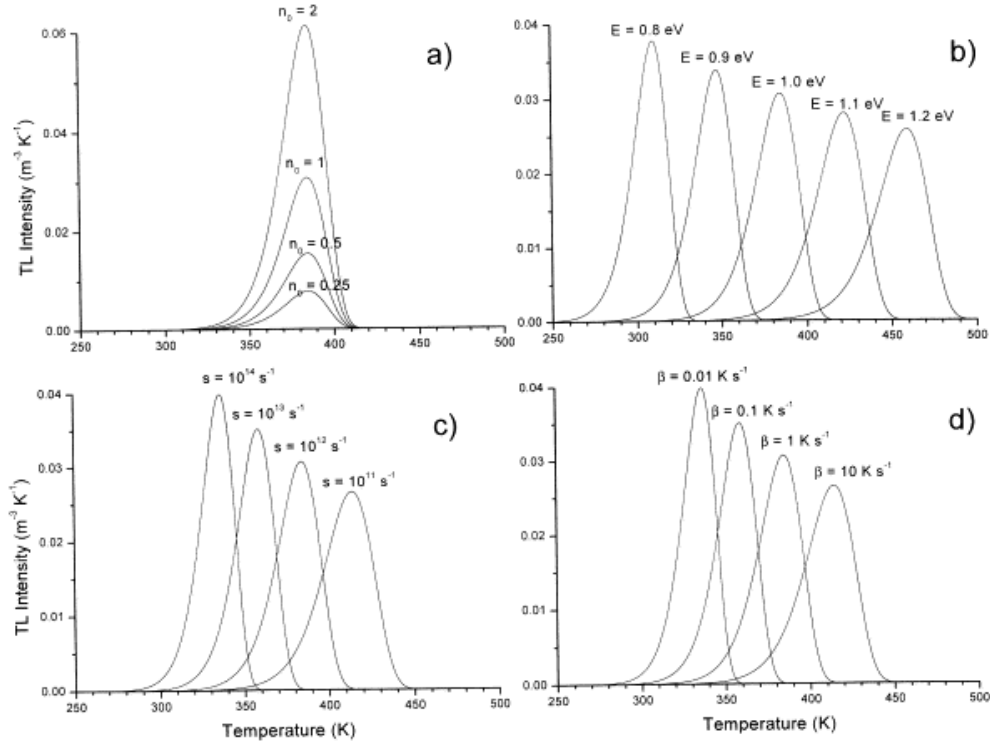


Figure 6. Properties of the Randall–Wilkins first-order TL equation, showing: (a) variation with n_0 , the concentration of trapped charge carriers after irradiation; (b) the variation with E , the activation energy; (c) the variation with s , the escape frequency; (d) the variation with β , the heating rate. Parameter values: $n_0=1 \text{ m}^{-3}$; $E=1 \text{ eV}$; $s=1 \times 10^{12} \text{ s}^{-1}$, $\beta=1 \text{ K/s}$ of which one parameter is varied while the others are kept constant [16].

It is worthwhile to note that of the four parameters the activation energy E and the frequency factor s are the main physical parameters. They are called the trapping parameters and are fixed by the properties of the trapping centre. The other two parameters can be chosen by the experimenter by choosing a certain dose (n_0) and by read-out of the signal at a certain heating rate β . Investigation of a new TL material will therefore start with studying the glow peak behavior under variation of the absorbed dose and the heating rate.

The evaluation of Eqn.(23) is hampered by the fact that the integral on the right-hand side is not elementary in the case of linear heating. This integral cannot be solved analytically, but can be found by successive integration by parts to be equal to [17]

$$F(T, E) = T \exp(-E/kT) \sum_{n=1}^{\infty} \left(\frac{kT}{E} \right)^n (-1)^n n! \quad (26)$$

By keeping only the first two terms in this approximation, the integral can be approximated by

$$F(T, E) = \frac{kT^2}{E} \exp(-E/kT) \left(\frac{1-2kT}{E} \right) \quad (27)$$

In practical applications it is convenient to describe the glow peak in terms of parameters which are easy to derive experimentally, namely the intensity of peak at the maximum I_m and the temperature at the maximum T_m . Therefore, by using this approximation to the integral and by further using the condition for the temperature T_m of the maximum TL intensity equation (24), Kitis et al. [18] have shown that Eqn.(23) can be quite accurately approximated by

$$I(T) = I_m \exp \left[1 + \frac{E}{kT} \frac{T - T_m}{T_m} - \frac{T^2}{T_m^2} \exp \left\{ \frac{E}{kT} \frac{T - T_m}{T_m} \right\} (1 - \Delta) - \Delta_m \right] \quad (28)$$

with $\Delta = 2kT/E$ and $\Delta_m = 2kT_m/E$. On the other hand, by keeping a lot of terms in the above approximation, Bos et.al. [19] were approximated the following first-order TL glow curve expression,

$$I(T) = n_0 s \exp\left(-\frac{E}{kT}\right) \exp \left[-\frac{s kT^2}{\beta E} \exp\left(-\frac{E}{kT}\right) * (0.9920 - 1.620 \frac{kT}{E_a}) \right] \quad (29)$$

2.8 Second-order kinetics

Garlick and Gibson [20] considered the possibility that retrapping dominates, i.e. $mA_n \ll (N-n)A_h$. Further they assume that the trap is far from saturation, i.e. $N \gg n$ and $n=m$. With these assumptions, Eqn.(17) becomes

$$I(t) = -\frac{dn}{dt} = s \frac{A_n}{NA_h} n^2 \exp\left\{-\frac{E}{kT}\right\} \quad (30)$$

We see that now dn/dt is proportional to n^2 which means a second-order reaction. With the additional assumption of equal probabilities of recombination and retrapping, $A_n = A_h$, integration of Eqn.(30) gives

$$I(T) = \frac{n_0^2 s}{N \beta} \exp\left\{-\frac{E}{kT}\right\} \left[1 + \frac{n_0 s}{N \beta} \int_{T_0}^T \exp\left\{-\frac{E}{kT'}\right\} dT' \right]^{-2} \quad (31)$$

This is the Garlick–Gibson TL equation for second-order kinetics. The main feature of this curve is that it is nearly symmetric, with the high temperature half of the curve slightly broader than the low temperature half. This can be understood from the consideration of the fact that in a second-order reaction significant concentrations of released electrons are retrapped before they recombine, in this way giving rise to a delay in the luminescence emission and spreading out of the emission over a wider temperature range.

The initial concentration n_0 appears here not merely as a multiplicative constant as in the first-order case, so that its variation at different dose levels change the shape of the whole curve. This is illustrated in Fig.7(a). It is seen that T_m decreases as n_0 increases. It can be derived [21] that the temperature shift can be approximated by

$$T_1 - T_2 \approx T_1 T_2 \frac{k}{E} \ln f \quad (32)$$

where T_1 is the temperature of maximum intensity at a certain dose and T_2 the temperature of maximum intensity at f times higher dose. With the parameter values of Fig.7(a) the shift is 25 K. When $E=1$ eV, $T_1=400$ K and the absorbed dose is increased by a factor 1000, which is easy to realise experimentally, a temperature shift of 77 K can be expected. From Eqn.(32) it follows further that for a given increase of the dose the shallower the trap, i.e., the smaller E , the larger the peak shift. Fig.7(b) illustrates the variation in size and position of a second-order peak as function of E , in Fig.7(c) as function of s/N , and in Fig.7(d) as function of the heating rate. The area under the curve is, as in the case of first-order kinetics, proportional to the initial concentration n_0 but the peak height is no longer directly proportional to the peak area, although the deviation is small.

Also for second-order kinetics the glow peak shape, Eqn.(31) can be approximated with a function written in terms of maximum peak intensity I_m and the maximum peak temperature T_m [18]

$$I(T) = 4I_m \exp\left(\frac{E}{kT} \frac{T - T_m}{T_m}\right) \times \left[\frac{T^2}{T_m^2} (1 - \Delta) \exp\left\{ \frac{E}{kT} \frac{T - T_m}{T_m} \right\} + 1 + \Delta_m \right]^{-2} \quad (33)$$

with Δ and Δ_m the same meaning as in Eqn.(28).

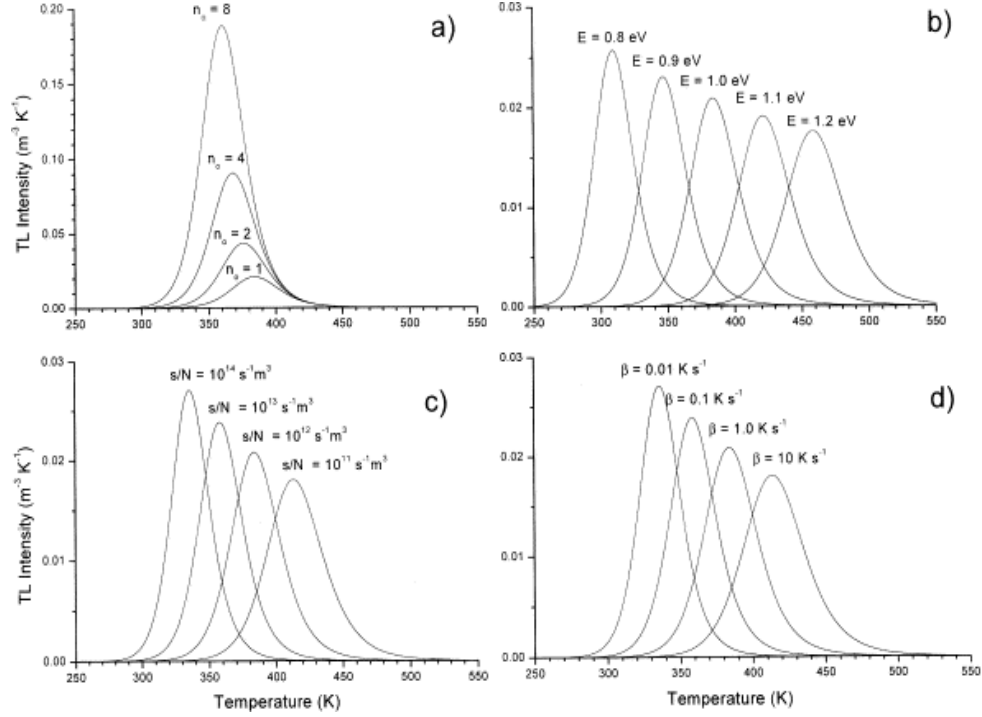


Figure 7. Properties of the Garlick–Gibson second-order TL equation, showing: (a) variation with n_0 , the concentration of trapped charge carriers after irradiation; (b) the variation with E , the activation energy; (c) the variation with s/N ; (d) the variation with β , the heating rate. Parameter values: $n_0=1 \text{ m}^{-3}$; $E=1 \text{ eV}$; $s/N=1 \times 10^{12} \text{ s}^{-1} \text{ m}^3$, $\beta=1 \text{ K/s}$ of which one parameter is varied while the others are kept constant [16].

2.9 General-order kinetics

The first- and second-order forms of the TL equation have been derived with the use of specific, simplifying assumptions. However, when these simplifying assumptions do not hold, the TL peak will fit neither first- nor the second-order kinetics. May and Partridge [22] used for this case an empirical expression for general-order TL kinetics, namely

$$I(t) = -\frac{dn}{dt} = n^b s' \exp\left\{-\frac{E}{kT}\right\} \quad (34)$$

where s' has the dimension of $m^{3(b-1)} \text{ s}^{-1}$ and b is defined as the general-order parameter and is not necessarily 1 or 2. Integration of Eqn.(34) for $b \neq 1$ yields

$$I(T) = \frac{s''}{\beta} n_0 \exp\left\{-\frac{E}{kT}\right\} \left[1 + (b-1) \frac{s''}{\beta} \int_{T_0}^T \exp\left\{-\frac{E}{kT'}\right\} dT' \right]^{-b/(b-1)} \quad (35)$$

where now $s'' = s' n_0^{b-1}$ with unit s^{-1} . Eqn.(35) includes the second-order case ($b=2$) and reduces to Eqn.(23) when $b \rightarrow 1$. It should be noted that according to Eqn.(34) the dimension of s' should be $m^{3(b-1)} \text{ s}^{-1}$ that means that the dimension changes with the

order b which makes it difficult to interpret physically. Still, the general-order case is useful since intermediate cases can be dealt with and it smoothly goes to first- and second-orders when $b \rightarrow 1$ and $b \rightarrow 2$, respectively (see Fig.8).

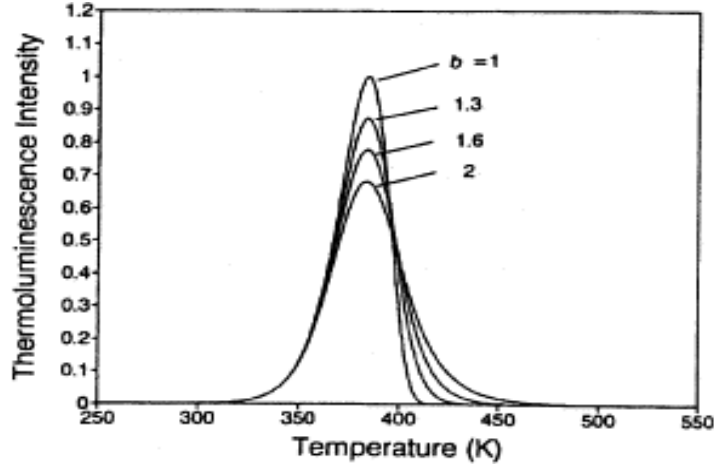


Figure 8. Comparison of first-order ($b=1$), second-order ($b=2$) and intermediate-order ($b=1.3$ and 1.6) TL peaks, with $E=1$ eV, $s=1 \times 10^{12} \text{ s}^{-1}$, $n_0=N=1 \text{ m}^{-3}$ and $\beta=1 \text{ K/s}$ [3].

In this model; the glow curve can be approximated by using the expression,

$$I(T) = n_0 s \exp\left(-\frac{E}{kT}\right) \left[1 + \left(-\frac{(b-1)s kT^2}{\beta E} \exp\left(-\frac{E}{kT}\right) * (0.9920 - 1.620 \frac{kT}{E}) \right)^{\frac{b}{b-1}} \right] \quad (36)$$

The equations (29) and (36) will be referred to as the Bos et.al. equations in this thesis and will be used to analyze the synthetic glow peaks obtained by Mathematica.

2.10 Advanced models

The one trap–one centre model shows all the characteristics of the phenomenon TL and explains the behavior of the glow peak shape under variation of the dose and heating rate. However, there is no existing TL material known that accurately is described by the simple model.

This does not mean that the simple model has no meaning. On the contrary, it can help us in the interpretation of many features which can be considered as variations of the one trap–one centre model. There is no room to discuss all the advanced (more realistic) models in detail. The text book of Chen and McKeever [3] for a deeper and quantitative treatment is referred. Here, only some models are very

briefly mentioned in order to get some idea about the complexity of the phenomenon in a real TL material.

In general, a real TL material will show more than one single electron trap. Not all the traps will be active in the temperature range in which the specimen is heated. A thermally disconnected trap is one which can be filled with electrons during irradiation but which has a trap depth which is much greater than the active trap such that when the specimen is heated only electrons trapped in the active trap (AT) and the shallow trap (ST) (see Fig.9(a)) are freed. Electrons trapped in the deeper levels are unaffected and thus this deep electron trap (indicated in Fig.9(a) with DET) is said to be thermally disconnected. But its existence has a bearing on the trapping filling and eventually on the shape of the glow peak [23].

In Section 2.3 it was assumed that the trapped electrons are released during heating while the trapped holes are stable in the recombination centre. A description in which the holes are released and recombine at a centre where the electrons are stable during heating is mathematically identical. However, the situation will change if both electrons and holes are released from their traps at the same time at the same temperature interval and the holes are being thermally released from the same centers as are acting as recombination sites for the thermally released electrons and vice versa (see Fig.9(b)). In this case Eqn.(10) is no longer valid. New differential equations should be drafted. Analysis of this complicated kinetic model reveals a TL glow curve which retains the simple Randall–Wilkins (Eqn.(23)) or Garlick–Gibson (Eqn.(31)) shape, depending upon the chosen values of the parameters. However, the E and s values used in Eqn.(23) and Eqn.(31) in order to obtain a fit on this complicated kinetic model need further interpretation.

Another process which might happen is a recombination without a transition of the electron into the conduction band (Fig.9(c)). Here the electron is thermally stimulated into an excited state from which a transition into the recombination centre is allowed. This means that the trap has to be in the proximity of a centre.

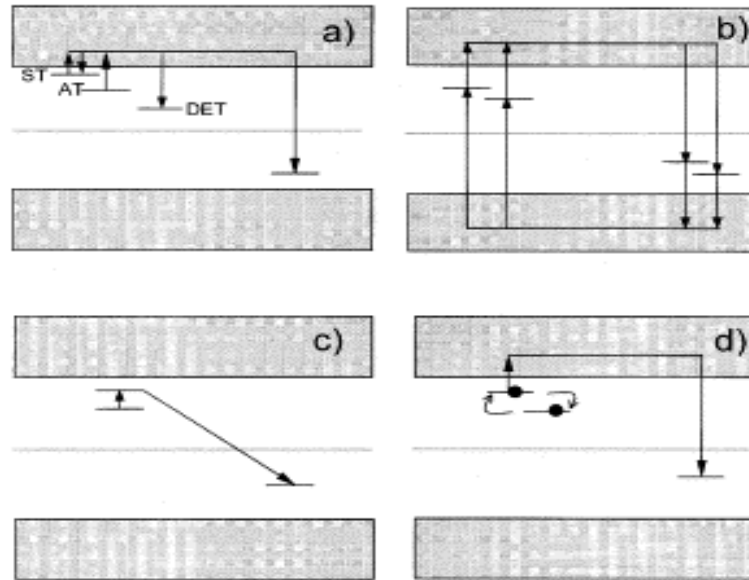


Figure 9. Advanced models describing the thermally stimulated release of trapped charged carriers including: (a) a shallow trap (ST), a deep electron trap (DET), and a active trap (AT); (b) two active traps and two recombination centers; (c) localized transitions; (d) defect interaction (trapping centre interacts with another defect) [3].

The transition probability may strongly depend on the distance between the two centers. Under certain assumptions an expression for the TL intensity can be derived [24] which has the same form as Eqn.(23) but with s replaced by a quantity related to the probability for recombination. This means that these localized transitions are governed by first-order kinetics.

Finally, we will mention the possibility that the defect which has trapped the electron is not stable but is involved in a reaction with another defect (Fig.9(d)). The result may be that at low temperature the trap depth is changing while the trapped electron concentration is stable. At higher temperatures electrons are involved in two processes: the escape to the conduction band and the defect reaction. Piters and Bos [25] have defect reactions incorporated into the rate equations and glow curves simulated. It appears that the simulated glow curves can be very well fitted by Eqn.(23). It is clear that (again) the fitting parameters do not have the simple meaning of trap depth and escape frequency.

2.11 Trapping Parameters Determination Methods

The determination of trapping parameters from thermoluminescence glow curves has been a subject of interest for half a century. There are various methods for

evaluating the trapping parameters from the glow curves [1-3, 26-31]. Some of them are initial rise method, variable heating, two heating, isothermal decay, peak shape, partial thermal cleaning and peak area methods.

When one glow peak is highly isolated from the others, the experimental methods such as initial rise, variable heating rates, isothermally decay, and peak shape methods are suitable methods to determine these parameters. However in most TL materials, the glow curve consists of several glow peaks. In case of overlapping glow peaks there are essentially two ways to obtain these parameters, the first one is the partial thermal cleaning method and the second one is the computer glow curve deconvolution program. In most cases, the partial thermal cleaning method can not be used to completely isolate the peak of interest without any perturbation on it. Therefore, the computer glow curve deconvolution (CGCD) program has become very popular method to evaluate trapping parameters from TL glow curves in recent years [2,19].

2.12 CGCD Method

As mentioned in previous paragraph, Computer Glow Curve Deconvolution (CGCD) is one of the most important methods to determine trapping parameters from TL glow curves. This method has the advantage over experimental methods in that they can be used in largely overlapping-peak glow curves without resorting to heat treatment.

It is well known that the CGCD is one of the most powerful techniques in the study of TL [2]. This technique is commonly used in the study dosimetric properties of TL dosimeters. The application of the CGCD technique for the decomposition of a composite TL glow curve into its individual glow peaks is widely applied since 1970 [32-34]. On the other hand, the obtained results from this method are highly dependent upon the input parameters which were used in the deconvolution program. For example, it is very important to decide correctly how many glow peaks there are in the glow curve during the analyses of the complex glow curves by computer curve fitting program and which of them have first- or general-order kinetics. In some cases, the best-fits can be obtained when different number of peaks is used in the curve fitting program instead of real number of glow peaks to be in the glow curve.

Therefore, it should be necessary to decide the correct number of glow peaks and their kinetic orders in the glow curve of synthetic quartz.

In this study, a CGCD program was used to analyze the glow curve of quartz. The program was developed at the Reactor Institute at Delft, The Netherlands [19]. This program is capable of simultaneously deconvoluting as many as nine glow peaks from glow curve. Two different models were used in the computer program. In the first model, the glow curve is approximated from first order TL kinetic by the expression,

$$I(T) = n_0 s \exp\left(-\frac{E}{kT}\right) \exp\left[-\frac{s kT^2}{\beta E} \exp\left(-\frac{E}{kT}\right) * \left(0.9920 - 1.620 \frac{kT}{E_a}\right)\right] \quad (29)$$

In the second model the glow curve is approximated with general order TL kinetics by using the expression,

$$I(T) = n_0 s \exp\left(-\frac{E}{kT}\right) \left[1 + \left(-\frac{(b-1)s kT^2}{\beta E} \exp\left(-\frac{E}{kT}\right) * \left(0.9920 - 1.620 \frac{kT}{E_a}\right)\right)^{\frac{b}{b-1}}\right] \quad (36)$$

where n_0 (m^{-3}) is the concentration of trapped electrons at $t=0$, s (s^{-1}) is the frequency factor for first-order and the pre-exponential factor for the general-order, E (eV) the activation energy, T (K) the absolute temperature, k (eVK^{-1}) Boltzmann's constant, β ($^{\circ}Cs^{-1}$) heating rate and b the kinetic order.

The summation of overall peaks and background contribution can lead to composite glow curve formula as shown below

$$I(T) = \sum_{i=1}^n I_i(T) + a + b \exp(T) \quad (37)$$

where $I(T)$ is the fitted total glow curve, a allows for the electronic noise contribution to the planchet and dosimeters infrared contribution to the background.

Starting from the above equation (37), the least square minimization procedure and also FOM (Figure of Merit) [35-36] was used to judge the fitting results as to whether they are good or not. i.e.

$$\text{FOM} = \sum_{i=1}^n \frac{|N_i(T) - I(T)|}{A} = \sum_{i=1}^n \frac{|\Delta N_i|}{A} \quad (38)$$

where $N_i(T)$ is the i -th experimental points (total $n=200$ data points), $I(T)$ is the i -th fitted points, and A is the integrated area of the fitted glow curve.

From many experiences [35-36], it can be said that if the values of the FOM are between 0.0% and 2.5% the fit is good, 2.5 % and 3.5% the fit is fair, and $> 3.5\%$ it is bad fit.

To have a graphic representation of the agreement between the experimental and fitted glow curves, the computer program also plots the function,

$$X(T) = \frac{N_i(T) - I_i(T)}{\sqrt{I_i(T)}} \quad (39)$$

which is a normal variable with an expected value 0 and $\sigma=1$ where $\sigma^2(T)=I_i(T)$.

2.13 Mathematica

Mathematica is a computational software program used in scientific, engineering, and mathematical fields and other areas of technical computing [37]. It was conceived by Stephen Wolfram and is developed by Wolfram Research of Champaign, Illinois [37]. Mathematica is split into two parts, the kernel and the front end. The kernel interprets expressions (Mathematica code) and returns result expressions. The *Mathematica* language was designed from the start to provide a clear and precise way of communicating ideas--from human to computer or from one human to another. Computer languages typically specify the operations in a rather low-level and literal way. But *Mathematica* is essentially unique among languages in common use because it operates at a much higher level, a level corresponding much more closely to normal human thinking.

Mathematica has emerged as an important tool in computer science and software development: its language component is widely used as a research, prototyping and interface environment. Therefore, *Mathematica* has become important in a remarkably wide range of fields over the years. *Mathematica* is used today throughout the sciences—physical, biological, social and other—and counts many of the world's foremost scientists among its enthusiastic supporters. It has

played a crucial role in many important discoveries, and has been the basis for thousands of technical papers.

In engineering, *Mathematica* has become a standard tool for both development and production, and by now many of the world's important new products rely at one stage or another in their design on *Mathematica*.

Whether they have tasks that involve numbers, formulas, functions, graphics, data, documents, or interfaces, *Mathematica* gives automatic access to by far the largest collection of algorithms ever assembled. Mathematica perform the arithmetic calculations in seconds that would take humans months or years to do unaided. Mathematica can perform all the usual calculus operations – such as integration, differentiation, series, limits, etc. But the essence of *Mathematica* is its language for describing and manipulating expressions. The numerical and symbolic computations by mathematica can be conducted and both two- and three-dimensional graphics, as well as counter and density plots can be produced. As a result, numeric of any precision, symbolic, or visualization- *Mathematica* is the ultimate computational tool, with system-wide technology to ensure reliability, ease-of-use, and performance.

2.13.1 Numerical Solution of Differential Equations by MATHEMATICA

The function NDSolve allows finding numerical solutions to differential equations by mathematica [37]. NDSolve handles both single differential equations, and sets of simultaneous differential equations. You can use NDSolve to solve systems of coupled differential equations. This finds a numerical solution to a pair of coupled equations. It can handle a wide range of *ordinary differential equations* as well as some *partial differential equations*. In a system of ordinary differential equations there can be any number of unknown functions y_i , but all of these functions must depend on a single “independent variable” x , which is the same for each function. Partial differential equations involve two or more independent variables [37].

`NDSolve[{ eqn1, eqn2, ... }, y, {x, xmin, xmax}]` \Rightarrow find a numerical solution for the function y with x in the range x_{min} to x_{max}

`NDSolve[{ eqn1, eqn2, ... }, {y1, y1, ...}, {x, xmin, xmax}]` \Rightarrow find numerical solutions for several functions y_i

NDSolve represents solutions for the functions y_i as InterpolatingFunction objects. The InterpolatingFunction objects provide approximations to the y_i over the range of values x_{min} to x_{max} for the independent variable x . NDSolve finds solutions iteratively. It starts at a particular value of x , then takes a sequence of steps, trying eventually to cover the whole range x_{min} to x_{max} . In order to get started, NDSolve has to be given appropriate initial or boundary conditions for the y_i and their derivatives. These conditions specify values for $y_i[x]$, and perhaps derivatives $y_i'[x]$, at particular points x . In general, at least for ordinary differential equations, the conditions you give can be at any x : NDSolve will automatically cover the range x_{min} to x_{max} .

When you use NDSolve, the initial or boundary conditions you give must be sufficient to determine the solutions for the y_i completely. When you use DSolve to find symbolic solutions to differential equations, you can get away with specifying fewer initial conditions. The reason is that DSolve automatically inserts arbitrary constants $C[i]$ to represent degrees of freedom associated with initial conditions that you have not specified explicitly. Since NDSolve must give a numerical solution, it cannot represent these kinds of additional degrees of freedom. As a result, you must explicitly give all the initial or boundary conditions that are needed to determine the solution. In a typical case, if you have differential equations with up to n^{th} derivatives, then you need to give initial conditions for up to $(n - 1)^{\text{th}}$ derivatives, or give boundary conditions at n points.

NDSolve has many methods for solving equations, but essentially all of them at some level work by taking a sequence of steps in the independent variable x , and using an adaptive procedure to determine the size of these steps. In general, if the solution appears to be varying rapidly in a particular region, then NDSolve will reduce the step size or change the method so as to be able to track the solution better. NDSolve follows the general procedure of reducing step size until it tracks solutions accurately. When NDSolve solves a particular set of differential equations, it always tries to choose a step size appropriate for those equations.

2.13.2 Numerical Solutions of Differential Equations of OTOR Model by Mathematica

As mentioned in the section 2.4, the simplest model in thermoluminescence phenomenon is the OTOR model which consists of two energy levels: the electron traps (ET) and the recombination center (RC) in the forbidden gap. The differential

equations governing the traffic of electrons between the electron trap level, the recombination center and the conduction band are:

$$\frac{dn_c}{dt} = ns \exp\left\{-\frac{E}{kT}\right\} - n_c(N-n)A_n - n_c mA_h \Rightarrow \text{Traffic of electrons in electron traps}$$

$$-\frac{dn}{dt} = np - n_c(N-n)A_n = ns \exp\left\{-\frac{E}{kT}\right\} - n_c(N-n)A_n \Rightarrow \text{Traffic of electrons in CB}$$

$$I(t) = -\frac{dm}{dt} = n_c mA_h = n_c(n + n_v)A_h \Rightarrow \text{Thermoluminescence Intensity (TL)}$$

Unfortunately these differential equations can not be solved in any closed form, and the solutions must be obtained numerically. Some of the results obtained by using Mathematica program with the OTOR model are shown in below examples after different values of kinetic parameters.

CHAPTER 3

NUMERICAL CALCULATIONS AND RESULTS

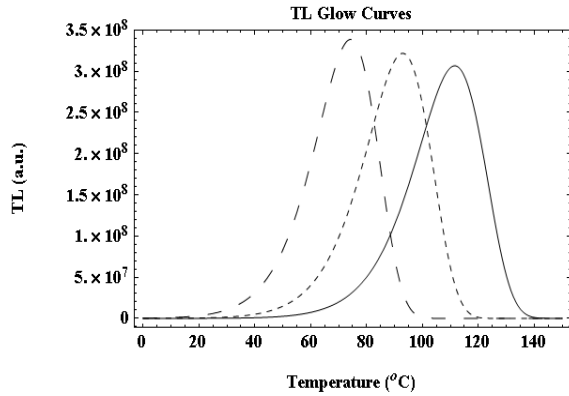
Example 1: The following simple programs in Mathematica solve the differential equations for the first, second and general-order kinetics with the initial value $n_o=N$. The command NDSolve is used to perform the numerical integration of the differential equation and the parameter x represents the temperature T ($^{\circ}\text{C}$) and the function $n[x]$ represents the electron concentration $n(T)$. The integration is generally carried out from a temperature of $T=0$ $^{\circ}\text{C}$ to $T=150$ $^{\circ}\text{C}$ (or up to 400 $^{\circ}\text{C}$ in some cases) and the command Plot is used to graph to result TL (T) of the numerical integration procedure. As seen from the numerically generated glow curves in below figures, the peak temperature position at maximum intensity (T_{max}) of the first-order TL glow curve ($A_n \ll A_h$) stays the same for the different values of the parameters n_o , but the maximum height (I_{max}) of the glow curve increases with increasing n_o , while the overall asymmetric shape of the TL glow curve remains the same. On the other hand, both the peak temperature (T_{max}) and maximum height (I_m) of the second ($A_n=A_h$) and general-order TL ($A_n \neq A_h$) glow curve change with the value of n_o .

(*This program describes the solution of differential equations of first order TL kinetics (b=1). It shows the effect of changing activation energy (E) on the first order thermoluminescence glow peaks. The kinetic parameters for calculations are shown in below;*)

$s = 10^{12}$; $E1 = 1$; $E2 = 0.95$; $E3 = 0.9$; $k = 8.617 \times 10^{-5}$; $n0 = 10^{10}$; $\beta = 1$;

TL1 = NDSolve[{n'[x] == -n[x] * s / β * E^{-E1 / (k * (273 + x))}}, n[0] == n0}, n, {x, 0, 150}];
 TL2 = NDSolve[{n'[x] == -n[x] * s / β * E^{-E2 / (k * (273 + x))}}, n[0] == n0}, n, {x, 0, 150}];
 TL3 = NDSolve[{n'[x] == -n[x] * s / β * E^{-E3 / (k * (273 + x))}}, n[0] == n0}, n, {x, 0, 150}];

Plot[{Evaluate[-n'[x] /. TL1], Evaluate[-n'[x] /. TL2], Evaluate[-n'[x] /. TL3]}, {x, 0, 150},
 PlotRange -> All, PlotLabel -> "TL Glow Curves", ImageSize -> 80x5, Frame -> True,
 FrameLabel -> {"Temperature (°C)", "TL (a.u.)"}, LabelStyle -> Directive[Bold, 12],
 PlotStyle -> {{Black}, {Dashed, Black}, {Dashing[Large], Black}}]

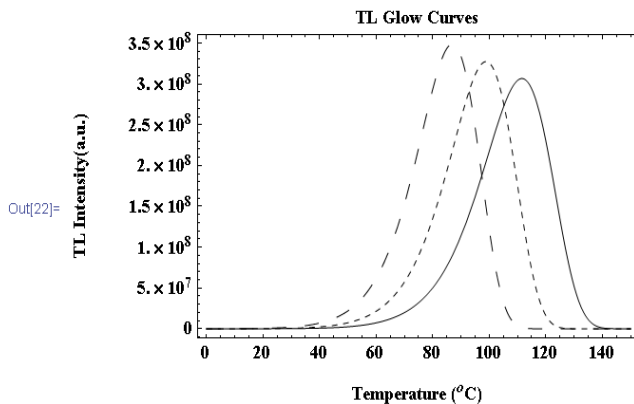


(*This program describes the solution of differential equations of first order TL kinetics (b=1). It shows the effect of changing frequency factor (s) on the first order thermoluminescence glow peaks. The kinetic parameters for calculations are shown in below;*)

$E1 = 1$; $s1 = 1 \times 10^{12}$; $s2 = 3 \times 10^{12}$; $s3 = 9 \times 10^{12}$; $k = 8.617 \times 10^{-5}$; $n0 = 10^{10}$; $\beta = 1$;

TL1 = NDSolve[{n'[x] == -n[x] * s1 / β * E^{-E1 / (k * (273 + x))}}, n[0] == n0}, n, {x, 0, 150}];
 TL2 = NDSolve[{n'[x] == -n[x] * s2 / β * E^{-E1 / (k * (273 + x))}}, n[0] == n0}, n, {x, 0, 150}];
 TL3 = NDSolve[{n'[x] == -n[x] * s3 / β * E^{-E1 / (k * (273 + x))}}, n[0] == n0}, n, {x, 0, 150}];

Plot[{Evaluate[-n'[x] /. TL1], Evaluate[-n'[x] /. TL2], Evaluate[-n'[x] /. TL3]}, {x, 0, 150},
 PlotRange -> All, PlotLabel -> "TL Glow Curves", ImageSize -> 80x5, Frame -> True,
 FrameLabel -> {"Temperature (°C)", "TL Intensity(a.u.)"}, LabelStyle -> Directive[Bold, 12],
 PlotStyle -> {{Black}, {Dashed, Black}, {Dashing[Large], Black}}]



ln[23]= (*This program describes the solution of differential equations of first order TL kinetics (b=1). It shows the effect of initial number of trapped electrons (n_0) in electron traps on the first order thermoluminescence glow peaks. The kinetic parameters for calculations are shown in below;*)

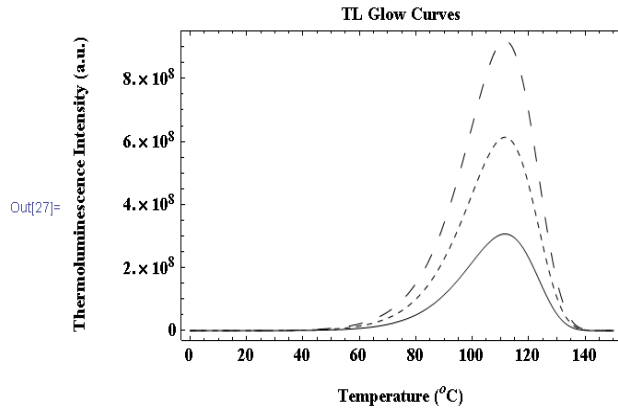
E1 = 1; s1 = 1 * 10^12; k = 8.617 * 10^-5; n1 = 1 * 10^10; n2 = 2 * 10^10; n3 = 3 * 10^10; β = 1;

TL1 = NDSolve[{n'[x] == -n[x] * s1 / β * E^(-E1 / (k * (273 + x))), n[0] == n1}, n, {x, 0, 150}];

TL2 = NDSolve[{n'[x] == -n[x] * s1 / β * E^(-E1 / (k * (273 + x))), n[0] == n2}, n, {x, 0, 150}];

TL3 = NDSolve[{n'[x] == -n[x] * s1 / β * E^(-E1 / (k * (273 + x))), n[0] == n3}, n, {x, 0, 150}];

Plot[{Evaluate[-n'[x] /. TL1], Evaluate[-n'[x] /. TL2], Evaluate[-n'[x] /. TL3]}, {x, 0, 150}, PlotRange -> All, PlotLabel -> "TL Glow Curves", ImageSize -> 80 * 5, Frame -> True, FrameLabel -> {"Temperature (°C)", "Thermoluminescence Intensity (a.u.)"}, LabelStyle -> Directive[Bold, 12], PlotStyle -> {{Black}, {Dashed, Black}, {Dashing[Large], Black}}]



ln[1]= (*This program describes the solution of differential equations of first order TL kinetics (b=1). It shows the effect of heating rate (β) on the first order thermoluminescence glow peaks. The kinetic parameters for calculations are shown in below;*)

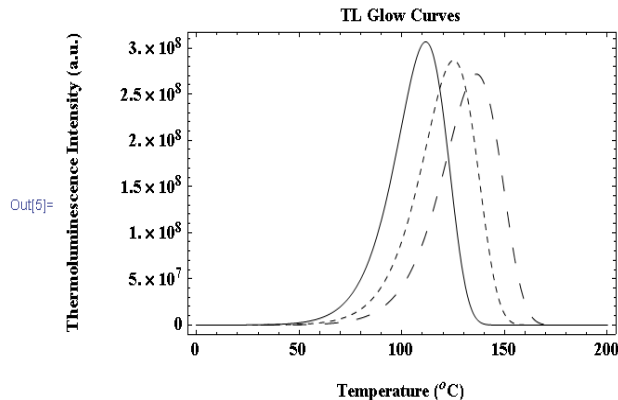
E1 = 1; s1 = 1 * 10^12; k = 8.617 * 10^-5; n1 = 1 * 10^10; β 1 = 1; β 2 = 3; β 3 = 7;

TL1 = NDSolve[{n'[x] == -n[x] * s1 / β 1 * E^(-E1 / (k * (273 + x))), n[0] == n1}, n, {x, 0, 200}];

TL2 = NDSolve[{n'[x] == -n[x] * s1 / β 2 * E^(-E1 / (k * (273 + x))), n[0] == n1}, n, {x, 0, 200}];

TL3 = NDSolve[{n'[x] == -n[x] * s1 / β 3 * E^(-E1 / (k * (273 + x))), n[0] == n1}, n, {x, 0, 200}];

Plot[{Evaluate[-n'[x] /. TL1], Evaluate[-n'[x] /. TL2], Evaluate[-n'[x] /. TL3]}, {x, 0, 200}, PlotRange -> All, PlotLabel -> "TL Glow Curves", ImageSize -> 80 * 5, Frame -> True, FrameLabel -> {"Temperature (°C)", "Thermoluminescence Intensity (a.u.)"}, LabelStyle -> Directive[Bold, 12], PlotStyle -> {{Black}, {Dashed, Black}, {Dashing[Large], Black}}]

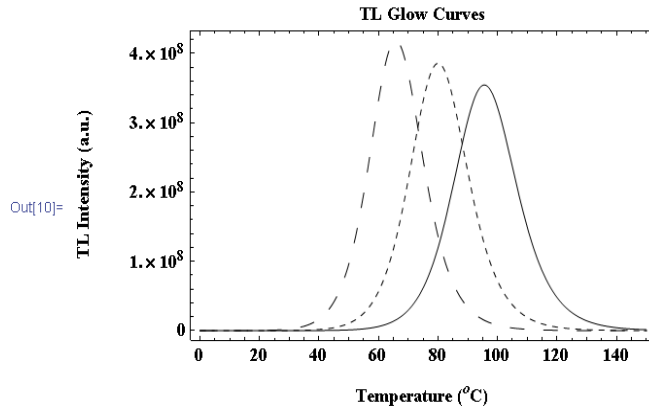


```
In[6]= (*This program describes the solution of differential equations of SECOND
ORDER TL kinetics (b=2). It shows the effect of changing frequency factor
(s) on the SECOND ORDER thermoluminescence glow peaks. The kinetic
paramaters for calculations are shown in below;*)
```

```
E1 = 1.6; s1 = 1 * 10^11; s2 = 1 * 10^12; s3 = 1 * 10^13; k = 8.617 * 10^-5; n0 = 10^10; β = 1;
```

```
TL1 = NDSolve[{n'[x] == -n[x] * n[x] * s1 / β * E^(-E1 / (k * (273 + x))), n[0] == n0}, n, {x, 0, 150}];
TL2 = NDSolve[{n'[x] == -n[x] * n[x] * s2 / β * E^(-E1 / (k * (273 + x))), n[0] == n0}, n, {x, 0, 150}];
TL3 = NDSolve[{n'[x] == -n[x] * n[x] * s3 / β * E^(-E1 / (k * (273 + x))), n[0] == n0}, n, {x, 0, 150}];
```

```
Plot[{Evaluate[-n'[x] /. TL1], Evaluate[-n'[x] /. TL2], Evaluate[-n'[x] /. TL3]}, {x, 0, 150},
PlotRange → All, PlotLabel → "TL Glow Curves", ImageSize → 80 × 5, Frame → True,
FrameLabel → {"Temperature (°C)", "TL Intensity (a.u.)"}, LabelStyle → Directive[Bold, 12],
PlotStyle → {{Black}, {Dashed, Black}, {Dashing[Large], Black}}]
```

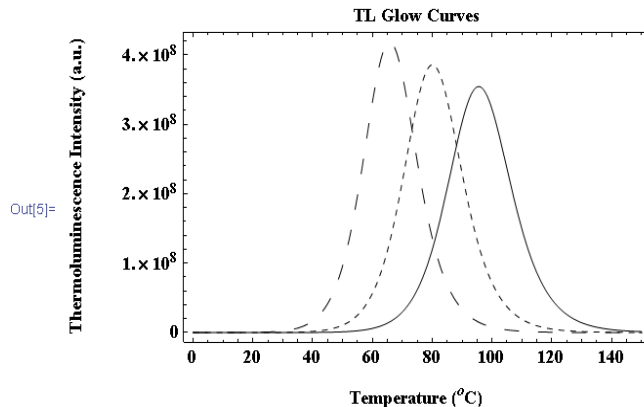


```
(*This program describes the solution of differential equations of SECOND
ORDER TL kinetics (b=2). It shows the effect of changing frequency factor
(s) on the SECOND ORDER thermoluminescence glow peaks. The kinetic
paramaters for calculations are shown in below;*)
```

```
E1 = 1.6; s1 = 1 * 10^11; s2 = 1 * 10^12; s3 = 1 * 10^13; k = 8.617 * 10^-5; n0 = 10^10; β = 1;
```

```
TL1 = NDSolve[{n'[x] == -n[x] * n[x] * s1 / β * E^(-E1 / (k * (273 + x))), n[0] == n0}, n, {x, 0, 150}];
TL2 = NDSolve[{n'[x] == -n[x] * n[x] * s2 / β * E^(-E1 / (k * (273 + x))), n[0] == n0}, n, {x, 0, 150}];
TL3 = NDSolve[{n'[x] == -n[x] * n[x] * s3 / β * E^(-E1 / (k * (273 + x))), n[0] == n0}, n, {x, 0, 150}];
```

```
Plot[{Evaluate[-n'[x] /. TL1], Evaluate[-n'[x] /. TL2], Evaluate[-n'[x] /. TL3]}, {x, 0, 150},
PlotRange → All, PlotLabel → "TL Glow Curves", ImageSize → 80 × 5, Frame → True,
FrameLabel → {"Temperature (°C)", "TL Intensity (a.u.)"}, LabelStyle → Directive[Bold, 12],
PlotStyle → {{Black}, {Dashed, Black}, {Dashing[Large], Black}}]
```



```

In[1]= (*This program describes the solution of differential equations of SECOND
ORDER TL kinetics (b=2). It shows the effect of initial number of trapped
electrons (n0)in electron traps on the SECOND ORDER thermoluminescence
glow peaks. The kinetic parameters for calculations are shown in below;*)

```

```

E1 = 1.7; s1 = 1*10^12; k = 8.617*10^-5; n1 = 1*10^10; n2 = 2*10^10; n3 = 3*10^10; β = 1;

```

```

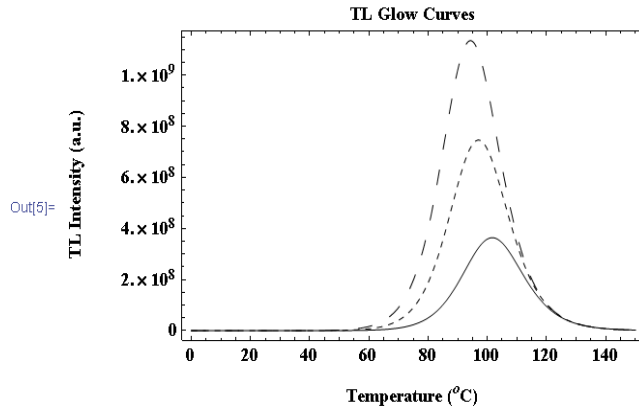
TL1 = NDSolve[{n'[x] == -n[x]*n[x]*s1/β*E^(-E1/(k*(273+x))), n[0] == n1}, n, {x, 0, 150}];
TL2 = NDSolve[{n'[x] == -n[x]*n[x]*s1/β*E^(-E1/(k*(273+x))), n[0] == n2}, n, {x, 0, 150}];
TL3 = NDSolve[{n'[x] == -n[x]*n[x]*s1/β*E^(-E1/(k*(273+x))), n[0] == n3}, n, {x, 0, 150}];

```

```

Plot[{Evaluate[-n'[x]/.TL1], Evaluate[-n'[x]/.TL2], Evaluate[-n'[x]/.TL3]}, {x, 0, 150},
PlotRange -> All, PlotLabel -> "TL Glow Curves", ImageSize -> 80*5, Frame -> True,
FrameLabel -> {"Temperature (°C)", "TL Intensity (a.u.)"}, LabelStyle -> Directive[Bold, 12],
PlotStyle -> {{Black}, {Dashed, Black}, {Dashing[Large], Black}}]

```



```

In[1]= (*This program describes the solution of differential equations of SECOND
ORDER TL kinetics (b=2). It shows the effect of heating rate (β)on the
SECOND ORDER thermoluminescence glow peaks. The kinetic paramaters for
calculations are shown in below;*)

```

```

E1 = 1.5; s1 = 1*10^12; k = 8.617*10^-5; n1 = 1*10^10; β1 = 1; β2 = 5; β3 = 25;

```

```

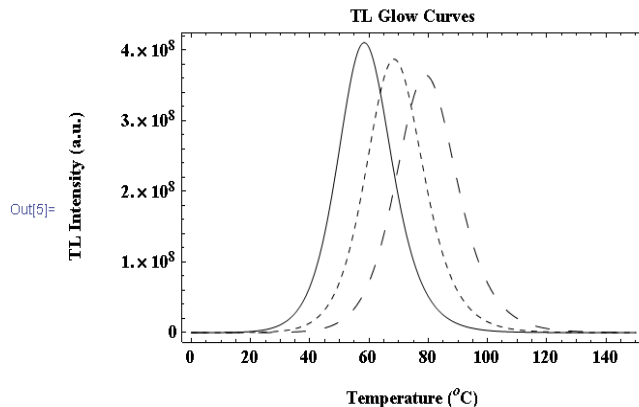
TL1 = NDSolve[{n'[x] == -n[x]*n[x]*s1/β1*E^(-E1/(k*(273+x))), n[0] == n1}, n, {x, 0, 150}];
TL2 = NDSolve[{n'[x] == -n[x]*n[x]*s1/β2*E^(-E1/(k*(273+x))), n[0] == n1}, n, {x, 0, 150}];
TL3 = NDSolve[{n'[x] == -n[x]*n[x]*s1/β3*E^(-E1/(k*(273+x))), n[0] == n1}, n, {x, 0, 150}];

```

```

Plot[{Evaluate[-n'[x]/.TL1], Evaluate[-n'[x]/.TL2], Evaluate[-n'[x]/.TL3]}, {x, 0, 150},
PlotRange -> All, PlotLabel -> "TL Glow Curves", ImageSize -> 80*5, Frame -> True,
FrameLabel -> {"Temperature (°C)", "TL Intensity (a.u.)"}, LabelStyle -> Directive[Bold, 12],
PlotStyle -> {{Black}, {Dashed, Black}, {Dashing[Large], Black}}]

```




```

In[1]= (*This program describes the solution of differential equations of GENERAL
ORDER TL kinetics (1<b≤2). It shows the effect of changing kinetic order
(b) on the GENERAL ORDER thermoluminescence glow peaks. The kinetic
paramaters for calculations are shown in below;*)

```

```

s = 10^14; E1 = 1.0; k = 8.617*10^-5; Nt = 1*10^10; n0 = 1*10^10; β = 1; b1 = 1.3; b2 = 1.5; b3 = 1.8;

```

```

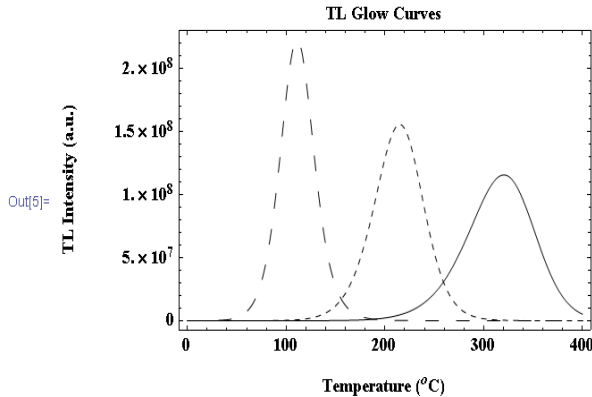
TL1 = NDSolve[{n'[x] == -(n[x]^b1) / Nt*s / β * E^(-E1 / (k*(273 + x))), n[0] == n0}, n, {x, 0, 400}];
TL2 = NDSolve[{n'[x] == -(n[x]^b2) / Nt*s / β * E^(-E1 / (k*(273 + x))), n[0] == n0}, n, {x, 0, 400}];
TL3 = NDSolve[{n'[x] == -(n[x]^b3) / Nt*s / β * E^(-E1 / (k*(273 + x))), n[0] == n0}, n, {x, 0, 400}];

```

```

Plot[{Evaluate[-n'[x] /. TL1], Evaluate[-n'[x] /. TL2], Evaluate[-n'[x] /. TL3]}, {x, 0, 400},
PlotRange -> All, PlotLabel -> "TL Glow Curves", ImageSize -> 80*5, Frame -> True,
FrameLabel -> {"Temperature (°C)", "TL Intensity (a.u.)"}, LabelStyle -> Directive[Bold, 12],
PlotStyle -> {{Black}, {Dashed, Black}, {Dashing[Large], Black}}]

```



```

In[1]= (*This program describes the solution of differential equations of GENERAL
ORDER TL kinetics (1<b≤2). It shows the effect of changing initial number
of trapped electrons (n0) in electron traps on the GENERAL ORDER
thermoluminescence glow peaks. The kinetic paramaters for calculations are shown in below;*)

```

```

s = 10^14; E1 = 1.0; k = 8.617*10^-5; Nt = 1*10^10; n1 = 1*10^10; n2 = 0.75*10^10; n3 = 0.5*10^10;
β = 1; b1 = 1.5;

```

```

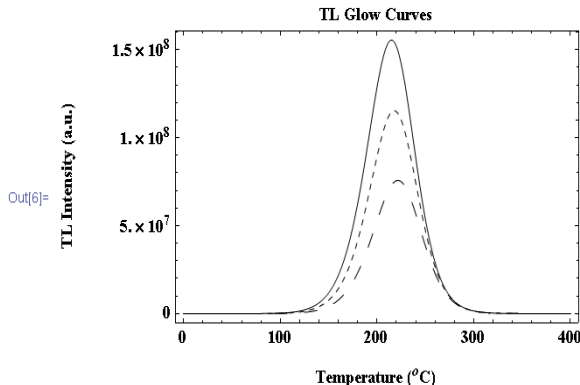
TL1 = NDSolve[{n'[x] == -(n[x]^b1) / Nt*s / β * E^(-E1 / (k*(273 + x))), n[0] == n1}, n, {x, 0, 400}];
TL2 = NDSolve[{n'[x] == -(n[x]^b1) / Nt*s / β * E^(-E1 / (k*(273 + x))), n[0] == n2}, n, {x, 0, 400}];
TL3 = NDSolve[{n'[x] == -(n[x]^b1) / Nt*s / β * E^(-E1 / (k*(273 + x))), n[0] == n3}, n, {x, 0, 400}];

```

```

Plot[{Evaluate[-n'[x] /. TL1], Evaluate[-n'[x] /. TL2], Evaluate[-n'[x] /. TL3]}, {x, 0, 400},
PlotRange -> All, PlotLabel -> "TL Glow Curves", ImageSize -> 80*5, Frame -> True,
FrameLabel -> {"Temperature (°C)", "TL Intensity (a.u.)"}, LabelStyle -> Directive[Bold, 12],
PlotStyle -> {{Black}, {Dashed, Black}, {Dashing[Large], Black}}]

```



Example 2: The following Mathematica programs integrate the differential equations for the OTOR model after different kinetic parameters. The command Plot is used to graph the functions $n_c(T)$, $n(T)$, $n_h(T)$ and $TL(T)$. The graphs in below figures show the results from using different A_n/A_h ratios. Note that when the $A_n=0.01A_h$, the probability coefficient A_h of the free electrons in the conduction band recombining in the RC is 100 x larger than the probability coefficient A_n of being retrapped in the electron trap. It can be easily assumed that the first-order kinetic will be satisfied under these conditions. The calculated TL glow curves have indeed represents the characteristic shape of the first-order glow curve under these circumstances. When A_n becomes equal to A_h , the probability coefficient A_h of recombining in the RC is equal to the retrapping probability coefficient A_n , which satisfies the second-order glow curves under this circumstances. If the $A_n=100x A_h$, the probability coefficient A_h of recombining in the RC is 100 x smaller than the retrapping probability coefficient A_n . In this case, the heavy retrapping is dominant and thereupon the intensity of TL glow curve being distributed over a much larger temperature region. As seen from the graphs in below figures, the concentrations of trapped electrons $n(T)$ in electron traps and holes $n_h(T)$ in RC decrease, simultaneously. On the other hand, the graph $n_c(T)$ shows that the concentration of free electrons in the conduction band increases up to a certain temperature which depends on the input kinetic parameters and then decreases with increasing temperature. Note that the peak temperatures of $n_c(T)$ and TL glow curve are different from each other.

```

In[8]:= (*This program describes the solution of differential equations of OTOR
        model. The kinetic parameters for calculations are shown in below;*)

k = 8.617*10^-5; Tm = 200; s = 1*10^12; El = 1.0; beta = 1; Nt = 1*10^10; Ah = 1*10^-7; An = 0.0001

sol = NDSolve[{nl'[x] == -nl[x] * s / beta * E^(-El / (k * (273 + x))) + An * (Nt - nl[x]) * nc[x] / beta,
nc'[x] == -nl'[x] - Ah * nc[x] * (nl[x] + nc[x]) / beta, nh'[x] == nl'[x] + nc'[x], nl[0] == Nt,
nc[0] == 0, nh[0] == nl[0] + nc[0]}, {nl, nc, nh}, {x, 0, Tm}];

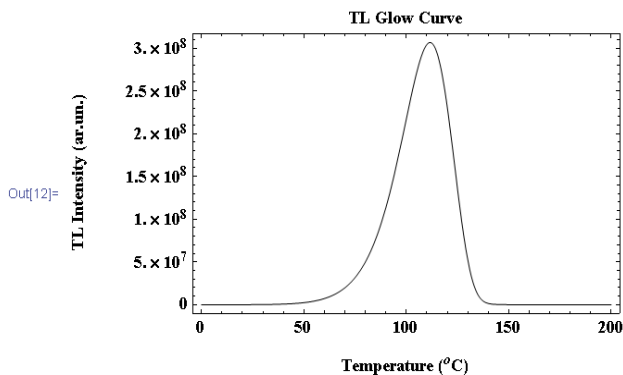
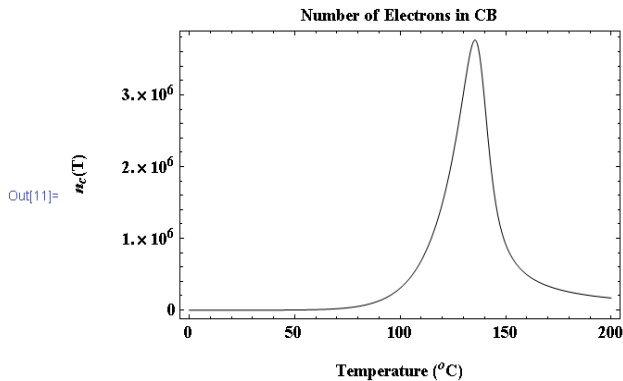
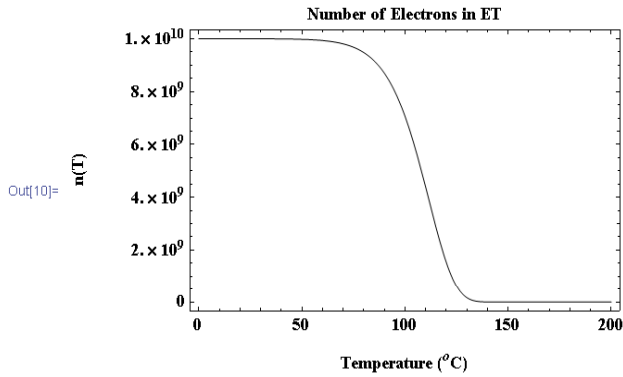
Plot[Evaluate[nl[x] /. sol], {x, 0, Tm}, PlotRange -> All, PlotLabel -> "Number of Electrons in ET",
ImageSize -> 80*5, Frame -> True, FrameLabel -> {"Temperature (°C)", "n(T)"},
LabelStyle -> Directive[Bold, 12], PlotStyle -> {{Black}}]

Plot[Evaluate[nc[x] /. sol], {x, 0, Tm}, PlotRange -> All, PlotLabel -> "Number of Electrons in CB",
ImageSize -> 80*5, Frame -> True, FrameLabel -> {"Temperature (°C)", "nc(T)"},
LabelStyle -> Directive[Bold, 12], PlotStyle -> {{Black}}]

Plot[Evaluate[-nh'[x] /. sol], {x, 0, Tm}, PlotRange -> All, PlotLabel -> "TL Glow Curve",
ImageSize -> 80*5, Frame -> True, FrameLabel -> {"Temperature (°C)", "TL Intensity (ar.un.)"},
LabelStyle -> Directive[Bold, 12], PlotStyle -> {{Black}}]

Clear[sol, nl, nc, nh, El, s, Nt, k, Ah, An]

```



```

In[1]:= (*This program describes the solution of differential equations of OTOR model. The
kinetic paramaters for calculations are shown in below;*)

k = 8.617*10^-5; Tm = 200; s = 1*10^12; E1 = 1.0; beta = 1; Nt = 1*10^10; Ah = 1*10^-7; An = 1*Ah;

sol = NDSolve[{nl'[x] == -nl[x]*s/beta*E^(-E1/(k*(273+x))) + An*(Nt - nl[x])*nc[x]/beta,
nc'[x] == -nl'[x] - Ah*nc[x]*(nl[x] + nc[x])/beta, nh'[x] == nl'[x] + nc'[x], nl[0] == Nt,
nc[0] == 0, nh[0] == nl[0] + nc[0]}, {nl, nc, nh}, {x, 0, Tm}];

Plot[Evaluate[nl[x] /. sol], {x, 0, Tm}, PlotRange -> All, PlotLabel -> "Number of Electrons in ET",
ImageSize -> 80*5, Frame -> True, FrameLabel -> {"Temperature (°C)", "n(T)"},
LabelStyle -> Directive[Bold, 12], PlotStyle -> {{Black}}]

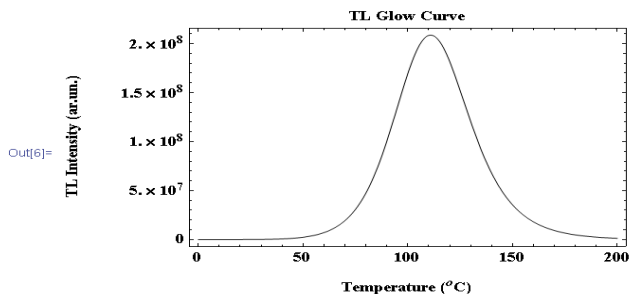
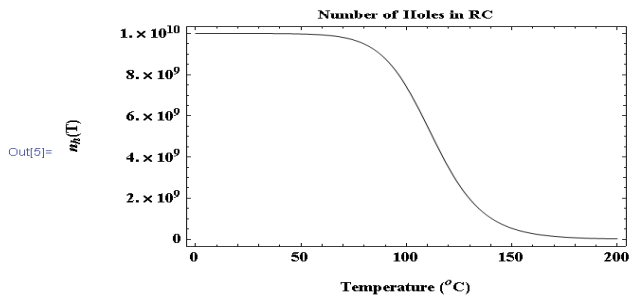
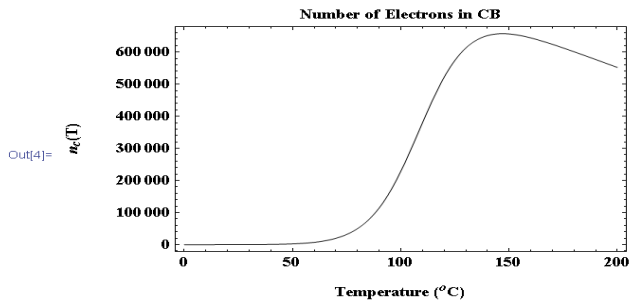
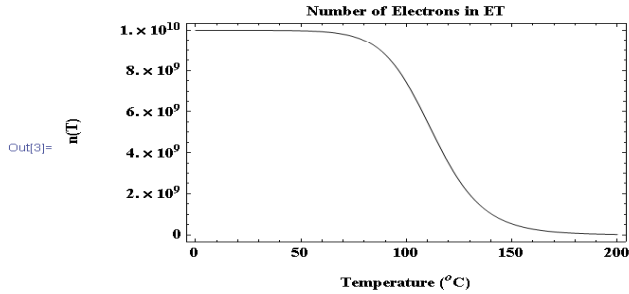
Plot[Evaluate[nc[x] /. sol], {x, 0, Tm}, PlotRange -> All, PlotLabel -> "Number of Electrons in CB",
ImageSize -> 80*5, Frame -> True, FrameLabel -> {"Temperature (°C)", "nc(T)"},
LabelStyle -> Directive[Bold, 12], PlotStyle -> {{Black}}]

Plot[Evaluate[nh[x] /. sol], {x, 0, Tm}, PlotRange -> All, PlotLabel -> "Number of Holes in RC",
ImageSize -> 80*5, Frame -> True, FrameLabel -> {"Temperature (°C)", "nh(T)"},
LabelStyle -> Directive[Bold, 12], PlotStyle -> {{Black}}]

Plot[Evaluate[-nh'[x] /. sol], {x, 0, Tm}, PlotRange -> All, PlotLabel -> "TL Glow Curve",
ImageSize -> 80*5, Frame -> True, FrameLabel -> {"Temperature (°C)", "TL Intensity (ar.un.)"},
LabelStyle -> Directive[Bold, 12], PlotStyle -> {{Black}}]

Clear[sol, nl, nc, nh, E1, s, Nt, k, Ah, An]

```



```

In[1]:= (*This program describes the solution of differential equations of OTOR model. The
kinetic paramaters for calculations are shown in below;*)

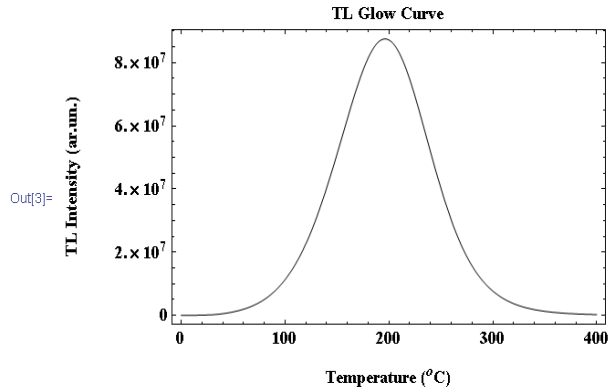
k = 8.617*10^-5; Tm = 400; s = 1*10^12; E1 = 1.0; β = 1; Nt = 1*10^10; Ah = 1*10^-7; An = 1000*Ah;

sol = NDSolve[{nl'[x] == -nl[x]*s/β*E^(-E1/(k*(273+x))) + An*(Nt - nl[x])*nc[x]/β,
nc'[x] == -nl'[x] - Ah*nc[x]*(nl[x] + nc[x])/β, nh'[x] == nl'[x] + nc'[x], nl[0] == Nt,
nc[0] == 0, nh[0] == nl[0] + nc[0]}, {nl, nc, nh}, {x, 0, Tm}];

Plot[Evaluate[-nh'[x]/.sol], {x, 0, Tm}, PlotRange -> All, PlotLabel -> "TL Glow Curve",
ImageSize -> 80*5, Frame -> True, FrameLabel -> {"Temperature (°C)", "TL Intensity (ar.un.)"},
LabelStyle -> Directive[Bold, 12], PlotStyle -> {{Black}}]

Clear[sol, nl, nc, nh, E1, s, Nt, k, Ah, An]

```



```
(*This program describes the solution of differential equations of OTOR model. The
kinetic paramaters for calculations are shown in below;*)
```

```
k = 8.617*10^-5; Tm = 250;
s1 = 1*10^12; s2 = 1*10^12; s3 = 1*10^12;
E1 = 1.0; E2 = 1.05; E3 = 1.1;
β1 = 1; β2 = 1; β3 = 1;
Nt1 = 1*10^10; Nt2 = 1*10^10; Nt3 = 1*10^10;
Ah1 = 1*10^-7; Ah2 = 1*10^-7; Ah3 = 1*10^-7;
An1 = 1*Ah1; An2 = 1*Ah2; An3 = 1*Ah3;

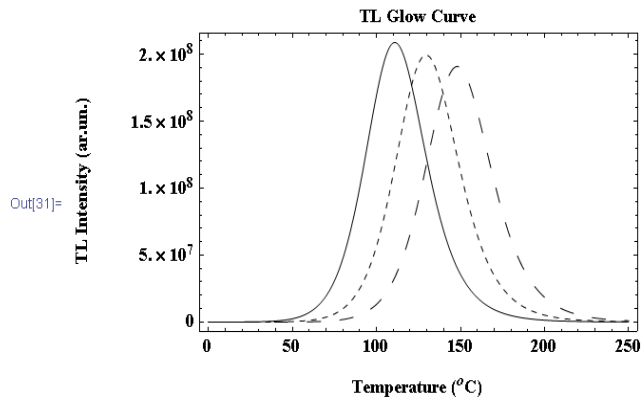
sol1 = NDSolve[{n1'[x] == -n1[x]*s1/β1*E^(-E1/(k*(273+x))) + An1*(Nt1 - n1[x])*nc1[x]/β1,
nc1'[x] == -n1'[x] - Ah1*nc1[x]*(n1[x] + nc1[x])/β1, nh1'[x] == n1'[x] + nc1'[x],
n1[0] == Nt1, nc1[0] == 0, nh1[0] == n1[0] + nc1[0]}, {n1, nc1, nh1}, {x, 0, Tm}];

sol2 = NDSolve[{n2'[x] == -n2[x]*s2/β2*E^(-E2/(k*(273+x))) + An2*(Nt2 - n2[x])*nc2[x]/β2,
nc2'[x] == -n2'[x] - Ah2*nc2[x]*(n2[x] + nc2[x])/β2, nh2'[x] == n2'[x] + nc2'[x],
n2[0] == Nt2, nc2[0] == 0, nh2[0] == n2[0] + nc2[0]}, {n2, nc2, nh2}, {x, 0, Tm}];

sol3 = NDSolve[{n3'[x] == -n3[x]*s3/β3*E^(-E3/(k*(273+x))) + An3*(Nt3 - n3[x])*nc3[x]/β3,
nc3'[x] == -n3'[x] - Ah3*nc3[x]*(n3[x] + nc3[x])/β3, nh3'[x] == n3'[x] + nc3'[x],
n3[0] == Nt3, nc3[0] == 0, nh3[0] == n3[0] + nc3[0]}, {n3, nc3, nh3}, {x, 0, Tm}];

Plot[{Evaluate[-nh1'[x]/.sol1], Evaluate[-nh2'[x]/.sol2], Evaluate[-nh3'[x]/.sol3]},
{x, 0, Tm}, PlotRange -> All, PlotLabel -> "TL Glow Curve", ImageSize -> 80*5, Frame -> True,
FrameLabel -> {"Temperature (°C)", "TL Intensity (ar.un.)"}, LabelStyle -> Directive[Bold, 12],
PlotStyle -> {{Black}, {Dashed, Black}, {Dashing[Large], Black}}]

Clear[sol1, n1, nc1, nh1, E1, s1, Nt1, β1, Ah1, An1, sol2, n2, nc2, nh2, E2, s2, Nt2, β2, Ah2,
An2, sol3, n3, nc3, nh3, E3, s3, Nt3, β3, Ah3, An3]
```



```
In[49]= (*This program describes the solution of differential equations of OTOR model. The
kinetic paramaters for calculations are shown in below;*)
```

```

k = 8.617*10^-5; Tm = 300;
s1 = 1*10^12; s2 = 1*10^12; s3 = 1*10^12;
E1 = 1.0; E2 = 1.0; E3 = 1.0;
β1 = 1; β2 = 1; β3 = 1;
Nt1 = 1*10^10; Nt2 = 1*10^10; Nt3 = 1*10^10;
Ah1 = 1*10^-7; Ah2 = 1*10^-7; Ah3 = 1*10^-7;
An1 = 0.1*Ah1; An2 = 10*Ah2; An3 = 1000*Ah3;

sol1 = NDSolve[{n1'[x] == -n1[x] * s1 / β1 * E^(-E1 / (k * (273 + x))) + An1 * (Nt1 - n1[x]) * nc1[x] / β1,
nc1'[x] == -n1'[x] - Ah1 * nc1[x] * (n1[x] + nc1[x]) / β1, nh1'[x] == n1'[x] + nc1'[x],
n1[0] == Nt1, nc1[0] == 0, nh1[0] == n1[0] + nc1[0]}, {n1, nc1, nh1}, {x, 0, Tm}];

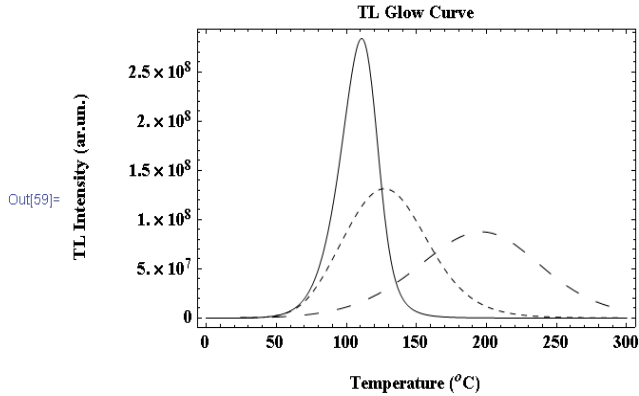
sol2 = NDSolve[{n2'[x] == -n2[x] * s2 / β2 * E^(-E2 / (k * (273 + x))) + An2 * (Nt2 - n2[x]) * nc2[x] / β2,
nc2'[x] == -n2'[x] - Ah2 * nc2[x] * (n2[x] + nc2[x]) / β2, nh2'[x] == n2'[x] + nc2'[x],
n2[0] == Nt2, nc2[0] == 0, nh2[0] == n2[0] + nc2[0]}, {n2, nc2, nh2}, {x, 0, Tm}];

sol3 = NDSolve[{n3'[x] == -n3[x] * s3 / β3 * E^(-E3 / (k * (273 + x))) + An3 * (Nt3 - n3[x]) * nc3[x] / β3,
nc3'[x] == -n3'[x] - Ah3 * nc3[x] * (n3[x] + nc3[x]) / β3, nh3'[x] == n3'[x] + nc3'[x],
n3[0] == Nt3, nc3[0] == 0, nh3[0] == n3[0] + nc3[0]}, {n3, nc3, nh3}, {x, 0, Tm}];

Plot[{Evaluate[-nh1'[x] /. sol1], Evaluate[-nh2'[x] /. sol2], Evaluate[-nh3'[x] /. sol3]},
{x, 0, Tm}, PlotRange -> All, PlotLabel -> "TL Glow Curve", ImageSize -> 80*5, Frame -> True,
FrameLabel -> {"Temperature (°C)", "TL Intensity (ar.un.)"}, LabelStyle -> Directive[Bold, 12],
PlotStyle -> {{Black}, {Dashed, Black}, {Dashing[Large], Black}}]

Clear[sol1, n1, nc1, nh1, E1, s1, Nt1, β1, Ah1, An1, sol2, n2, nc2, nh2, E2, s2, Nt2, β2, Ah2,
An2, sol3, n3, nc3, nh3, E3, s3, Nt3, β3, Ah3, An3]

```



```
In[133]= (*This program describes the solution of differential equations of OTOR model. The
kinetic parameters for calculations are shown in below;*)
```

```

k = 8.617*10^-5; Tm = 250;
s1 = 1*10^12; s2 = 1*10^12; s3 = 1*10^12;
E1 = 1.0; E2 = 1.0; E3 = 1.0;
β1 = 1; β2 = 10; β3 = 50;
Nt1 = 1*10^10; Nt2 = 1*10^10; Nt3 = 1*10^10;
Ah1 = 1*10^-7; Ah2 = 1*10^-7; Ah3 = 1*10^-7;
An1 = 0.1*Ah1; An2 = 0.1*Ah2; An3 = 0.1*Ah3;

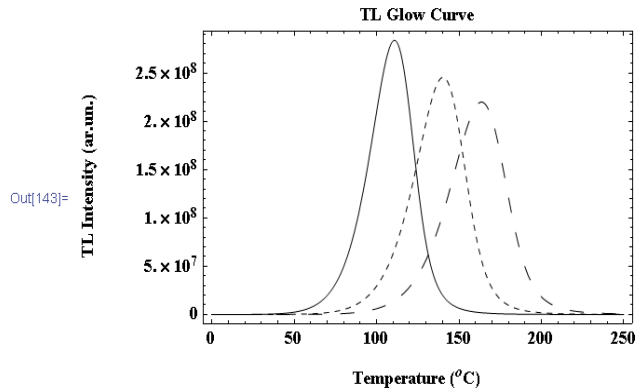
sol1 = NDSolve[{n1'[x] == -n1[x]*s1/β1*E^(-E1/(k*(273+x))) + An1*(Nt1 - n1[x])*nc1[x]/β1,
nc1'[x] == -n1'[x] - Ah1*nc1[x]*(n1[x] + nc1[x])/β1, nh1'[x] == n1'[x] + nc1'[x],
n1[0] == Nt1, nc1[0] == 0, nh1[0] == n1[0] + nc1[0]}, {n1, nc1, nh1}, {x, 0, Tm}];

sol2 = NDSolve[{n2'[x] == -n2[x]*s2/β2*E^(-E2/(k*(273+x))) + An2*(Nt2 - n2[x])*nc2[x]/β2,
nc2'[x] == -n2'[x] - Ah2*nc2[x]*(n2[x] + nc2[x])/β2, nh2'[x] == n2'[x] + nc2'[x],
n2[0] == Nt2, nc2[0] == 0, nh2[0] == n2[0] + nc2[0]}, {n2, nc2, nh2}, {x, 0, Tm}, MaxSteps -> 20000];

sol3 = NDSolve[{n3'[x] == -n3[x]*s3/β3*E^(-E3/(k*(273+x))) + An3*(Nt3 - n3[x])*nc3[x]/β3,
nc3'[x] == -n3'[x] - Ah3*nc3[x]*(n3[x] + nc3[x])/β3, nh3'[x] == n3'[x] + nc3'[x],
n3[0] == Nt3, nc3[0] == 0, nh3[0] == n3[0] + nc3[0]}, {n3, nc3, nh3}, {x, 0, Tm}, MaxSteps -> 20000];

Plot[{Evaluate[-nh1'[x] /. sol1], Evaluate[-nh2'[x] /. sol2], Evaluate[-nh3'[x] /. sol3]},
{x, 0, Tm}, PlotRange -> All, PlotLabel -> "TL Glow Curve", ImageSize -> 80*5, Frame -> True,
FrameLabel -> {"Temperature (°C)", "TL Intensity (ar.un.)"}, LabelStyle -> Directive[Bold, 12],
PlotStyle -> {{Black}, {Dashed, Black}, {Dashing[Large], Black}}]

Clear[sol1, n1, nc1, nh1, E1, s1, Nt1, β1, Ah1, An1, sol2, n2, nc2, nh2, E2, s2, Nt2, β2, Ah2,
An2, sol3, n3, nc3, nh3, E3, s3, Nt3, β3, Ah3, An3]
```




```

In[169]= (*This program describes the solution of differential equations of OTOR model. The
kinetic paramaters for calculations are shown in below;*)

k = 8.617*10^-5; Tm = 200;
s1 = 1*10^12; s2 = 1*10^12; s3 = 1*10^12;
E1 = 1.0; E2 = 1.0; E3 = 1.0;
β1 = 1; β2 = 1; β3 = 1;
Nt1 = 1*10^10; Nt2 = 1*10^10; Nt3 = 1*10^10;
Ah1 = 1*10^-7; Ah2 = 1*10^-7; Ah3 = 1*10^-7;
An1 = 1*Ah1; An2 = 1*Ah2; An3 = 1*Ah3;

sol1 = NDSolve[{n1'[x] == -n1[x]*s1/β1*E^(-E1/(k*(273+x))) + An1*(Nt1 - n1[x])*nc1[x]/β1,
nc1'[x] == -n1[x] - Ah1*nc1[x]*(n1[x] + nc1[x])/β1, nh1'[x] == n1'[x] + nc1'[x],
n1[0] == Nt1, nc1[0] == 0, nh1[0] == n1[0] + nc1[0]}, {n1, nc1, nh1}, {x, 0, Tm}];

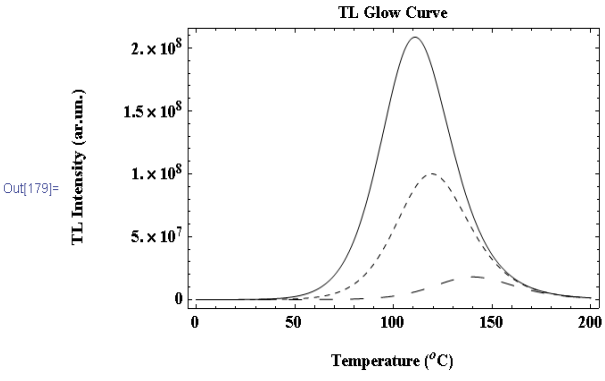
sol2 = NDSolve[{n2'[x] == -n2[x]*s2/β2*E^(-E2/(k*(273+x))) + An2*(Nt2 - n2[x])*nc2[x]/β2,
nc2'[x] == -n2'[x] - Ah2*nc2[x]*(n2[x] + nc2[x])/β2, nh2'[x] == n2'[x] + nc2'[x],
n2[0] == 0.5*Nt2, nc2[0] == 0, nh2[0] == n2[0] + nc2[0]}, {n2, nc2, nh2}, {x, 0, Tm}, MaxSteps -> 20000];

sol3 = NDSolve[{n3'[x] == -n3[x]*s3/β3*E^(-E3/(k*(273+x))) + An3*(Nt3 - n3[x])*nc3[x]/β3,
nc3'[x] == -n3'[x] - Ah3*nc3[x]*(n3[x] + nc3[x])/β3, nh3'[x] == n3'[x] + nc3'[x],
n3[0] == 0.1*Nt3, nc3[0] == 0, nh3[0] == n3[0] + nc3[0]}, {n3, nc3, nh3}, {x, 0, Tm}, MaxSteps -> 20000];

Plot[{Evaluate[-nh1'[x] /. sol1], Evaluate[-nh2'[x] /. sol2], Evaluate[-nh3'[x] /. sol3]},
{x, 0, Tm}, PlotRange -> All, PlotLabel -> "TL Glow Curve", ImageSize -> 80x5, Frame -> True,
FrameLabel -> {"Temperature (°C)", "TL Intensity (ar.un.)"}, LabelStyle -> Directive[Bold, 12],
PlotStyle -> {{Black}, {Dashed, Black}, {Dashing[Large], Black}}]

Clear[sol1, n1, nc1, nh1, E1, s1, Nt1, β1, Ah1, An1, sol2, n2, nc2, nh2, E2, s2, Nt2, β2, Ah2,
An2, sol3, n3, nc3, nh3, E3, s3, Nt3, β3, Ah3, An3]

```



The glow curves of TL materials are in most cases complex curves which consisting of many overlapping glow peaks. The deconvolution of this type complex glow curves into their individual glow peaks is widely applied for dosimetric applications and also to evaluate some of the kinetic parameters such as E_a , s , n_o and b . As mentioned in chapter 2, Bos et al [19] was developed analytical equations for the first (Equation 29) and general-order (Equation 36) kinetic peaks to analyze the experimental glow curves by computer glow curve deconvolution program (CGCD).

In this thesis, the curve fitting (deconvolution) procedure was performed by using commercially available software (TAMTAM) [19]. To compare the accuracy of expressions 29 and 36 with a synthetic reference glow peak, the exact solutions of the OTOR model were performed by Mathematica program after different kinetic parameters and then the numerical results of the solutions were stored in the computer. They were then analyzed by the computer glow curve fitting program (TAMTAM) and the results of curve fitting (deconvolution) program were compared with the input kinetic parameters that were used in numerical solutions. The parameters n_o , E_a , s and b are free parameters used in the expressions to fit numerical data. The results are shown in Tables 1-5. The column labeled FOM is obtained by using the TAMTAM program which was explained in chapter 2, in detail. The FOM value gives an estimate about the accuracy of used expressions (29 and 36) that were developed by Bos et.al [19]. It is important to note that the FOM values are very sensitive to small changes in the kinetic parameters used in expressions 29 and 36. Some of the selected glow curves after analyzing by curve fitting program (CGCD) are shown in figures 10-20, where the calculated $I(T)$ from equation (36) is compared with the numerical solutions of differential equations of TL. In the given study, approximately two hundred exact numerical solutions based on the OTOR model were solved after different kinetic parameters and then they compared with the approximated TL equation 36 to obtain its accuracy.

Table 1. The below table includes some of the input parameters which were used in numerical simulated TL glow curves and obtained kinetic parameters after their analyzing by curve fitting program.

Input Parameters : ($\beta=0,1$ °C/s, $n_0=1*10^8$ m⁻³, $E_a=1$ eV, $s=1x10^{12}$ s⁻¹)							
			n₀	E_a	s	b	FOM
sin1	n _o = N _t	A _n =0.0001A _h	0,9985*10 ⁷	1	9,989*10 ¹¹	1	0,01752
sin2	n _o =0,5 N _t		0,4992*10 ⁷	1	1,009*10 ¹²	1	0,03529
sin3	n _o = 0,1N _t		0,9974*10 ⁶	1,002	1,050*10 ¹²	1,003	0,17506
sin4	n _o = 0,01N _t		0,9916*10 ⁵	1,017	1,766*10 ¹²	1,046	1,19082
sin5	n _o = 0,001N _t		0,9770*10 ⁴	1,071	1,037*10 ¹³	1,312	3,61685
sin6	n _o = N _t	A _n =0.001A _h	0,9977*10 ⁷	1,001	1,039*10 ¹²	1,003	0,12867
sin7	n _o =0,5 N _t		0,4985*10 ⁷	1,003	1,093*10 ¹²	1,006	0,24998
sin8	n _o = 0,1N _t		0,9930*10 ⁶	1,014	1,582*10 ¹²	1,038	0,97125
sin9	n _o = 0,01N _t		0,9819*10 ⁵	1,064	8,406*10 ¹²	1,28	3,11114
sin10	n _o = 0,001N _t		0,9849*10 ⁴	1,058	3,660*10 ¹²	1,783	2,40515
sin11	n _o = N _t	A _n =0.01A _h	0,9931*10 ⁷	1,013	1,582*10 ¹²	1,037	0,95352
sin12	n _o =0,5 N _t		0,4950*10 ⁷	1,024	2,290*10 ¹²	1,074	1,82769
sin13	n _o = 0,1N _t		0,9823*10 ⁷	1,064	8,322*10 ¹²	1,278	3,05884
sin14	n _o = 0,01N _t		0,9878*10 ⁵	1,063	4,301*10 ¹²	1,79	2,08951
sin15	n _o = 0,001N _t		0,9944*10 ⁴	1,013	1,393*10 ¹¹	1,985	0,59666
sin16	n _o = N _t	A _n =0.1A _h	0,9821*10 ⁷	1,066	9,964*10 ¹²	1,296	3,1137
sin17	n _o =0,5 N _t		0,4908*10 ⁷	1,079	1,385*10 ¹³	1,45	3,27957
sin18	n _o = 0,1N _t		0,9890*10 ⁶	1,059	3,970*10 ¹²	1,874	1,94167
sin19	n _o = 0,01N _t		0,9970*10 ⁶	1,011	1,298*10 ¹¹	1,979	0,32298
sin20	n _o = 0,001N _t		0,9963*10 ⁴	1,003	1,066*10 ¹⁰	2,006	0,249895
sin21	n _o = N _t	A _n =A _h	0,9986*10 ⁷	1	9,989*10 ¹¹	2	0,00119
sin22	n _o =0,5 N _t		0,4993*10 ⁷	1	5,010*10 ¹¹	2	0,00135
sin23	n _o = 0,1N _t		0,9987*10 ⁶	1	1,001*10 ¹¹	2	0,003128
sin24	n _o = 0,01N _t		0,9985*10 ⁵	1	1,004*10 ¹⁰	2,001	0,01993
sin25	n _o = 0,001N _t		0,9968*10 ⁴	1,001	1,027*10 ⁹	2,007	0,15471
sin26	n _o = N _t	A _n =10A _h	1,017*10 ⁷	0,6137	9,748*10 ⁵	1,761	4,30322
sin27	n _o =0,5 N _t		0,5042*10 ⁷	0,9085	4,467*10 ⁹	2,091	2,13212
sin28	n _o = 0,1N _t		1,00*10 ⁷	0,9878	7,513*10 ⁹	2,022	0,33106
sin29	n _o = 0,01N _t		0,9987*10 ⁵	0,999	9,770*10 ⁸	2,003	0,03254
sin30	n _o = 0,001N _t		0,9970*10 ⁴	1,001	1,019*10 ⁸	2,005	0,07677
sin31	n _o = N _t	A _n =100A _h	0,9973*10 ⁷	0,4883	2,338	1,441	1,08002
sin32	n _o =0,5 N _t		0,505*10 ⁷	0,8933	3,704*10 ⁸	2,096	2,42142
sin33	n _o = 0,1N _t		1,01*10 ⁷	0,9865	7,533*10 ⁸	2,025	0,36549
sin34	n _o = 0,01N _t		0,9986*10 ⁵	0,9989	9,795*10 ⁶	2,003	0,03126
sin35	n _o = 0,001N _t		0,977*10 ⁴	1,001	1,022*10 ⁷	2,004	0,04358
sin36	n _o = N _t	A _n =1000A _h	0,9889*10 ⁷	0,4771	1,044*10 ³	1,412	0,58983
sin37	n _o =0,5 N _t		0,505*10 ⁷	0,8919	4,490*10 ⁷	2,098	2,42871
sin38	n _o = 0,1N _t		0,1*10 ⁷	0,9865	7,783*10 ⁷	2,025	0,36267
sin39	n _o = 0,01N _t		0,9984*10 ⁵	0,9989	9,820*10 ⁶	2,002	0,03065
sin40	n _o = 0,001N _t		0,9967*10 ⁴	1	1,014*10 ⁶	2,003	0,03315

Table 2. The below table includes some of the input parameters which were used in numerical simulated TL glow curves and obtained kinetic parameters after their analyzing by curve fitting program.

Input Parameters : ($\beta=1$ °C/s, $n_0=1*10^8$ m ⁻³ , $E_a=1$ eV, $s=1x10^{12}$ s ⁻¹)							
			n_0	E_a	s	b	FOM
sin41	$n_0= N_t$	$A_n=0.0001A_h$	$9,982*10^4$	1	$1,009*10^{12}$	1.000	0,06045
sin42	$n_0=0,5 N_t$		$4,989*10^4$	1,001	$1,019*10^{12}$	1.001	0,119444
sin43	$n_0= 0,1N_t$		$9,955*10^3$	1,005	$1,184*10^{12}$	1.011	0,498869
sin44	$n_0= 0,01N_t$		$9,843*10^2$	1,034	$1,104*10^{12}$	1,103	2,30209
sin45	$n_0= 0,001N_t$		$9,570*10^1$	1,103	$2,402*10^{13}$	1,527	6,0621
sin46	$n_0= N_t$	$A_n=0.001A_h$	$9,976*10^4$	1,002	$1,05*10^{12}$	1,003	0,168242
sin47	$n_0=0,5 N_t$		$4,983*10^4$	1,001	$1,115*10^{12}$	1,007	0,32029
sin48	$n_0= 0,1N_t$		$9,919*10^3$	1,016	$1,680*10^{12}$	1,045	1,158788
sin49	$n_0= 0,01N_t$		$9,777*10^2$	1,088	$1,547*10^{13}$	1,342	3,767716
sin50	$n_0= 0,001N_t$		$9,679*10^1$	1,087	$7,917*10^{12}$	1,925	4,363155
sin51	$n_0= N_t$	$A_n=0.01A_h$	$9,931*10^4$	1,014	$1,551*10^{12}$	1,038	0,972078
sin52	$n_0=0,5 N_t$		$4,95*10^4$	1,025	$2,223*10^{12}$	1,076	1,55778
sin53	$n_0= 0,1N_t$		$9,821*10^3$	1,065	$7,382*10^{12}$	1,28	3,105021
sin54	$n_0= 0,01N_t$		$9,856*10^2$	1,064	$3,853*10^{12}$	1,797	2,34306
sin55	$n_0= 0,001N_t$		$9,796*10^1$	1,034	$2,538*10^{11}$	2,101	2,153541
sin56	$n_0= N_t$	$A_n=0.1A_h$	$9,822*10^4$	1,066	$8,576*10^{12}$	1,296	3,11546
sin57	$n_0=0,5 N_t$		$4,908*10^4$	1,079	$1,158*10^{13}$	1,449	3,2837
sin58	$n_0= 0,1N_t$		$9,888*10^3$	1,061	$3,74*10^{12}$	1,808	1,971645
sin59	$n_0= 0,01N_t$		$9,85*10^2$	1,012	$1,312*10^{11}$	1,986	0,50893
sin60	$n_0= 0,001N_t$		$9,838*10^1$	1,015	$1,656*10^{10}$	2,101	1,433039
sin61	$n_0= N_t$	$A_n=A_h$	$9,987*10^4$	1	$9,99*10^{11}$	2	0,002988
sin62	$n_0=0,5 N_t$		$4,993*10^4$	1	$5,011*10^{11}$	2	0,004823
sin63	$n_0= 0,1N_t$		$9,985*10^3$	1	$1,002*10^{11}$	2,001	0,020159
sin64	$n_0= 0,01N_t$		$9,968*10^2$	1,001	$1,035*10^{11}$	2,007	0,156553
sin65	$n_0= 0,001N_t$		$9,860*10^1$	1,016	$1,517*10^9$	2,09	0,933721
sin66	$n_0= N_t$	$A_n=10A_h$	$1,016*10^5$	0,6132	$2,213*10^6$	1,765	4,352142
sin67	$n_0=0,5 N_t$		$1,000*10^4$	0,988	$7,743*10^9$	2,023	0,320373
sin68	$n_0= 0,1N_t$		$5,043*10^4$	0,9087	$5,511*10^9$	2,093	2,128989
sin69	$n_0= 0,01N_t$		$9,972*10^2$	1	$1,007*10^9$	2,008	0,061963
sin70	$n_0= 0,001N_t$		$9,871*10^1$	1,012	$1,34*10^8$	2,069	0,432317
sin71	$n_0= N_t$	$A_n=100A_h$	$9,951*10^4$	0,4866	$1,409*10^4$	1,442	1,117486
sin72	$n_0=0,5 N_t$		$5,049*10^4$	0,8936	$4,66*10^8$	2,098	0,250262
sin73	$n_0= 0,1N_t$		$1,000*10^4$	0,9852	$8,079*10^8$	2,03	0,360565
sin74	$n_0= 0,01N_t$		$9,971*10^2$	0,9994	$9,993*10^7$	2,006	0,033888
sin75	$n_0= 0,001N_t$		$9,59*10^2$	1,046	$2,572*10^6$	2,058	3,309812
sin76	$n_0= N_t$	$A_n=1000A_h$	$9,857*10^4$	0,4749	$3,053*10^3$	1,413	0,982541
sin77	$n_0=0,5 N_t$		$5,049*10^4$	0,8928	$5,766*10^7$	2,104	0,479272
sin78	$n_0= 0,1N_t$		$1,000*10^4$	0,9866	$8,02*10^7$	2,206	0,34047
sin79	$n_0= 0,01N_t$		$9,968*10^2$	0,9993	$9,919*10^6$	2,005	0,0191
sin80	$n_0= 0,001N_t$		$9,633*10^2$	1,035	$1,91*10^5$	2,346	2,22899

Table 3. The below table includes some of the input parameters which were used in numerical simulated TL glow curves and obtained kinetic parameters after their analyzing by curve fitting program.

Input Parameters : ($\beta=10$ °C/s, $n_0=1*10^8$ m ⁻³ , $E_a=1$ eV, $s=1*10^{12}$ s ⁻¹)							
			n_0	E_a	s	b	FOM
sin81	$n_0= N_t$	$A_n=0.0001A_h$	$9,964*10^4$	1,003	$1,1040*10^{12}$	1,006	0,366599
sin82	$n_0= 0,5N_t$		$4,974*10^4$	1,007	$1,2324*10^{12}$	1,014	0,638702
sin83	$n_0= 0,1N_t$		$9,872*10^3$	1,027	$2,2456*10^{12}$	1,071	1,86222
sin84	$n_0= 0,01N_t$		$9,602*10^2$	1,088	$1,3449*10^{13}$	1,375	5,41131
sin85	$n_0= 0,001N_t$		$8,962*10^1$	1,246	$8,969*10^{14}$	2,665	12,5245
sin86	$n_0= N_t$	$A_n=0.001A_h$	$9,959*10^4$	1,005	$1,1490*10^{12}$	1,009	0,451479
sin87	$n_0= 0,5N_t$		$4,97*10^4$	1,009	$1,3217*10^{12}$	1,021	0,778231
sin88	$n_0= 0,1N_t$		$9,854*10^3$	1,034	$2,7155*10^{12}$	1,098	2,1807
sin89	$n_0= 0,01N_t$		$9,598*10^2$	1,099	$1,7098*10^{13}$	1,497	5,63614
sin90	$n_0= 0,001N_t$		$9,120*10^1$	1,212	$2,0417*10^{14}$	2,924	9,655409
sin91	$n_0= N_t$	$A_n=0.01A_h$	$9,922*10^4$	1,016	$1,6144*10^{12}$	1,044	1,133825
sin92	$n_0= 0,5N_t$		$4,943*10^4$	1,028	$2,3140*10^{12}$	1,086	1,76497
sin93	$n_0= 0,1N_t$		$9,79*10^3$	1,069	$7,3080*10^{12}$	1,303	3,455167
sin94	$n_0= 0,01N_t$		$9,705*10^2$	1,083	$5,8648*10^{12}$	1,905	3,93445
sin95	$n_0= 0,001N_t$		$9,327*10^1$	1,112	$2,1575*10^{12}$	2,978	5,706505
sin96	$n_0= N_t$	$A_n=0.1A_h$	$9,820*10^4$	1,066	$7,4557*10^{12}$	1,297	3,147088
sin97	$n_0= 0,5N_t$		$4,906*10^4$	1,079	$9,8648*10^{12}$	1,451	3,335493
sin98	$n_0= 0,1N_t$		$9,867*10^3$	1,061	$3,2187*10^{12}$	1,821	2,165499
sin99	$n_0= 0,01N_t$		$9,824*10^2$	1,026	$1,9185*10^{11}$	2,075	1,663309
sin100	$n_0= 0,001N_t$		$9,404*10^1$	1,075	$7,4943*10^{10}$	2,824	3,911959
sin101	$n_0= N_t$	$A_n=1A_h$	$9,985*10^4$	1	$1,0090*10^{12}$	2,001	0,020097
sin102	$n_0= 0,5N_t$		$4,992*10^3$	1	$2,5132*10^{11}$	2,001	0,037954
sin103	$n_0= 0,1N_t$		$9,968*10^3$	1,001	$1,032*10^{11}$	2,007	0,154555
sin104	$n_0= 0,01N_t$		$9,854*10^2$	1,011	$1,3554*10^{10}$	2,078	0,880246
sin105	$n_0= 0,001N_t$		$9,477*10^1$	1,067	$5,2421*10^9$	2,709	5,77433
sin106	$n_0= N_t$	$A_n=10A_h$	$1,015*10^5$	0,6128	$5,0758*10^6$	1,77	4,36158
sin107	$n_0= 0,5N_t$		$5,041*10^4$	0,9084	$6,7310*10^9$	2,096	2,096301
sin108	$n_0= 0,1N_t$		$9,986*10^3$	0,9886	$8,1395*10^9$	2,028	0,268975
sin109	$n_0= 0,01N_t$		$0,9876*10^2$	1,007	$1,2174*10^9$	2,062	0,553988
sin110	$n_0= 0,001N_t$		$9,537*10^1$	1,057	$359,419*10^6$	2,579	4,81497
sin111	$n_0= N_t$	$A_n=100A_h$	$9,920*10^4$	0,4845	$3,974*10^4$	1,443	1,09401
sin112	$n_0= 0,5N_t$		$5,046*10^4$	0,8939	$5,926*10^8$	2,102	2,35898
sin113	$n_0= 0,1N_t$		$9,987*10^3$	0,9872	$8,1606*10^8$	2,029	0,30344
sin114	$n_0= 0,01N_t$		$9,89*10^2$	1,005	$1,1380*10^8$	2,049	0,425015
sin115	$n_0= 0,001N_t$		$9,59*10^1$	1,046	$2,5906*10^7$	24,6	3,71238
sin116	$n_0= N_t$	$A_n=1000A_h$	$9,811*10^4$	0,4723	$8,866*10^3$	1,413	0,544288
sin117	$n_0= 0,5N_t$		$5,044*10^4$	0,8926	$8,1606*10^8$	2,105	2,371826
sin118	$n_0= 0,1N_t$		$9,984*10^4$	0,987	$8,3470*10^7$	2,029	0,315627
sin119	$n_0= 0,01N_t$		$9,896*10^2$	1,003	$1,0853*10^7$	2,036	0,260166
sin120	$n_0= 0,001N_t$		$9,636$	1,036	$1,9434*10^6$	2,35	2,53095

Table 4. The below table includes some of the input parameters which were used in numerical simulated TL glow curves and obtained kinetic parameters after their analyzing by curve fitting program.

Input Parameters : ($\beta=50$ °C/s, $n_0=1*10^8$ m ⁻³ , $E_a=1$ eV, $s=1x10^{12}$ s ⁻¹)							
			n_0	E_a	s	b	FOM
sin121	$n_0= N_t$	$A_n=0.0001A_h$	$9,919*10^4$	1,014	$1,4903*10^{12}$	1,032	1,10692
sin122	$n_0= 0,5N_t$		$4,941 *10^4$	1,024	$1,9916*10^{12}$	1,062	1,70397
sin123	$n_0= 0,1N_t$		$9,731 *10^3$	1,062	$9,4780*10^{12}$	1,216	3,77195
sin124	$n_0= 0,01N_t$		$9,223*10^2$	1,164	$0,8218*10^{12}$	1,922	10,7743
sin125	$n_0= 0,001N_t$		$8,728*10^1$	1,469	$1,1925*10^{17}$	6,535	14,3807
sin126	$n_0= N_t$	$A_n=0.001A_h$	$9,916*10^4$	1,015	$1,5356*10^{12}$	1,036	1,1664
sin127	$n_0= 0,5N_t$		$4,939*10^4$	1,026	$2,0937*10^{12}$	1,068	1,779
sin128	$n_0= 0,1N_t$		$9,725*10^3$	1,065	$6,1655*10^{12}$	1,234	3,8872
sin129	$n_0= 0,01N_t$		$9,243*10^2$	1,166	$0,8301*10^{12}$	1,998	10,5358
sin130	$n_0= 0,001N_t$		$8,845*10^1$	1,406	$1,6767*10^{16}$	6,529	12,2644
sin131	$n_0= N_t$	$A_n=0.01A_h$	$9,891*10^4$	1,024	$1,9916*10^{12}$	1,067	1,6248
sin132	$n_0= 0,5N_t$		$4,922*10^4$	1,039	$3,001*10^{12}$	1,123	2,3805
sin133	$n_0= 0,1N_t$		$9,701*10^3$	1,083	$9,6695*10^{12}$	1,389	4,4237
sin134	$n_0= 0,01N_t$		$9,388*10^2$	1,144	$0,2550*10^{12}$	2,319	8,1986
sin135	$n_0= 0,001N_t$		$9,091*10^1$	1,199	$0,0167*10^{12}$	5,928	8,1946
sin136	$n_0= N_t$	$A_n=0.1A_h$	$9,808*10^4$	1,068	$7,0920*10^{12}$	1,307	3,2752
sin137	$n_0= 0,5N_t$		$4,896*10^4$	1,08	$9,1979*10^{12}$	1,463	3,5249
sin138	$n_0= 0,1N_t$		$9,799*10^3$	1,068	$25,507*10^{12}$	1,85	2,7971
sin139	$n_0= 0,01N_t$		$9,559*10^2$	1,069	$5,7636*10^{11}$	2,44	5,394
sin140	$n_0= 0,001N_t$		$9,168*10^1$	1,114	$1,8068*10^{11}$	5,189	6,709
sin141	$n_0= N_t$	$A_n=1A_h$	$9,977*10^4$	1,001	$1,0191*10^{11}$	2,003	0,0905
sin142	$n_0= 0,5N_t$		$4,984*10^4$	1,001	$5,1632*10^{11}$	2,007	0,1662
sin143	$n_0= 0,1N_t$		$9,912*10^3$	1,006	$1,1871*10^{11}$	2,038	0,6604
sin144	$n_0= 0,01N_t$		$9,626*10^2$	1,045	$3,4012*10^{10}$	2,382	3,976
sin145	$n_0= 0,001N_t$		$9,208*10^1$	1,098	$9,9416*10^9$	4,639	5,95
sin146	$n_0= N_t$	$A_n=10A_h$	$1,014*10^5$	0,6129	$9,0656*10^6$	1,776	4,3475
sin147	$n_0= 0,5N_t$		$5,034*10^4$	0,9096	$7,8203*10^9$	2,101	2,0196
sin148	$n_0= 0,1N_t$		$9,938*10^3$	0,9922	$9,0859*10^9$	2,053	0,395
sin149	$n_0= 0,01N_t$		$9,674*10^2$	1,036	$2,3088*10^9$	2,313	3,5332
sin150	$n_0= 0,001N_t$		$9,245*10^1$	1,086	$6,292*10^8$	4,137	4,8734
sin151	$n_0= N_t$	$A_n=100A_h$	$9,887*10^4$	0,483	$8,328*10^4$	1,445	1,1037
sin152	$n_0= 0,5N_t$		$8,039*10^4$	0,8943	$7,0239*10^8$	2,107	2,3256
sin153	$n_0= 0,1N_t$		$9,946*10^3$	0,9898	$8,8402*10^8$	2,049	0,3219
sin154	$n_0= 0,01N_t$		$9,714*10^2$	1,028	$1,8208*10^8$	2,248	1,3153
sin155	$n_0= 0,001N_t$		$9,276*10^1$	1,071	$3,982*10^7$	3,669	1,3739
sin156	$n_0= N_t$	$A_n=1000A_h$	$9,765*10^4$	0,4704	$1,869*10^4$	1,413	0,536
sin157	$n_0= 0,5N_t$		$5,037*10^4$	0,8931	$8,601*10^7$	2,11	2,3727
sin158	$n_0= 0,1N_t$		$9,946*10^3$	0,9888	$8,863*10^7$	2,043	0,2405
sin159	$n_0= 0,01N_t$		$9,746*10^2$	1,021	$1,509*10^7$	2,101	1,9024
sin160	$n_0= 0,001N_t$		$9,301*10^1$	1,054	$2,5715*10^6$	3,242	2,4996

Table 5: The below table includes some of the input parameters which were used in numerical simulated TL glow curves and obtained kinetic parameters after their analyzing by curve fitting program.

Input Parameters : ($\beta=100$ °C/s, $n_0=1*10^8$ m ⁻³ , $E_a=1$ eV, $s=1x10^{12}$ s ⁻¹)							
			n_0	E_a	s	b	FOM
sin161	$n_0= N_t$	$A_n=0.0001A_h$	$9,885*10^4$	1,023	$1,913*10^{12}$	1,089	1,6607
sin162	$n_0= 0,5N_t$		$4,917*10^4$	1,037	$2,798*10^{12}$	1,106	2,42993
sin163	$n_0= 0,1N_t$		$9,636*10^2$	1,081	$9,290*10^{12}$	1,326	5,01662
sin164	$n_0= 0,01N_t$		$9,004*10^2$	1,229	$3,720*10^{14}$	2,432	12,44617
sin165	$n_0= 0,001N_t$		$9,096*10^1$	1,506	$1,317*10^{17}$	10,81	8,75551
sin166	$n_0= N_t$	$A_n=0.001A_h$	$9,883*10^4$	1,024	$1,9522*10^{12}$	1,062	1,70044
sin167	$n_0= 0,5N_t$		$4,916*10^4$	1,038	$2,883*10^{12}$	1,111	2,481623
sin168	$n_0= 0,1N_t$		$9,633*10^3$	1,083	$9,669*10^{12}$	1,341	5,07991
sin169	$n_0= 0,01N_t$		$9,028*10^2$	1,228	$3,366*10^{14}$	2,49	11,84567
sin170	$n_0= 0,001N_t$		$9,173*10^1$	1,453	$2,741*10^{16}$	10,64	7,68958
sin171	$n_0= N_t$	$A_n=0.01A_h$	$9,863*10^4$	1,031	$2,408*10^{12}$	1,091	2,05303
sin172	$n_0= 0,5N_t$		$4,904*10^4$	1,048	$3,777*10^{12}$	1,159	2,90984
sin173	$n_0= 0,1N_t$		$9,625*10^3$	1,095	$1,254*10^{13}$	1,471	5,35799
sin174	$n_0= 0,01N_t$		$9,188*10^2$	1,195	$8,553*10^{13}$	27,64	9,21646
sin175	$n_0= 0,001N_t$		$9,372*10^1$	1,214	$1,8155*10^{13}$	9,19	4,75489
sin176	$n_0= N_t$	$A_n=0.1A_h$	$9,795*10^4$	1,07	$7,163*10^{12}$	1,318	3,43466
sin177	$n_0= 0,5N_t$		$4,886*10^4$	1,083	$9,197*10^{12}$	1,478	3,76562
sin178	$n_0= 0,1N_t$		$9,735*10^3$	1,077	$4,344*10^{12}$	1,9	3,58013
sin179	$n_0= 0,01N_t$		$9,391*10^2$	1,099	$1,220*10^{12}$	2,828	5,37231
sin180	$n_0= 0,001N_t$		$9,362*10^1$	1,085	$8,0377*10^{10}$	7,538	3,65081
sin181	$n_0= N_t$	$A_n=1A_h$	$9,968*10^4$	1,002	$1,0397*10^{12}$	2,007	0,188736
sin182	$n_0= 0,5N_t$		$4,976*10^4$	1,003	$5,373*10^{11}$	2,014	0,343823
sin183	$n_0= 0,1N_t$		$9,860*10^1$	1,012	$1,379*10^{11}$	2,079	1,2014
sin184	$n_0= 0,01N_t$		$9,472*10^2$	1,066	$5,0740*10^{10}$	2,697	3,859845
sin185	$n_0= 0,001N_t$		$9,325*10^1$	1,066	$4,631*10^9$	6,494	3,529098
sin186	$n_0= N_t$	$A_n=10A_h$	$10,12*10^4$	0,6133	$1,1875*10^7$	1,78	4,311816
sin187	$n_0= 0,5N_t$		$5,027*10^4$	0,9103	$8,47172*10^9$	2,107	1,934597
sin188	$n_0= 0,1N_t$		$9,893*10^3$	0,9966	$1,0142*10^{10}$	2,086	0,659989
sin189	$n_0= 0,01N_t$		$9,522*10^2$	1,05	$3,1478*10^9$	2,554	2,640746
sin190	$n_0= 0,001N_t$		$9,288*10^1$	1,06	$3,4879*10^8$	5,602	3,125251
sin191	$n_0= N_t$	$A_n=100A_h$	$9,867*10^4$	0,4827	$1,1469*10^5$	1,447	1,261145
sin192	$n_0= 0,5N_t$		$5,033*10^4$	0,8948	$7,6089*10^8$	2,112	2,276235
sin193	$n_0= 0,1N_t$		$9,908*10^3$	0,9933	$9,5706*10^8$	2,075	0,662469
sin194	$n_0= 0,01N_t$		$9,591*10^2$	1,044	$2,5075*10^8$	2,458	3,10024
sin195	$n_0= 0,001N_t$		$9,254*10^1$	1,051	$2,61667*10^7$	4,796	2,55594
sin196	$n_0= N_t$	$A_n=1000A_h$	$9,732*10^4$	0,4696	$2,584*10^4$	1,414	0,67626
sin197	$n_0= 0,5N_t$		$5,031*10^4$	0,8933	$9,224*10^7$	2,114	2,330667
sin198	$n_0= 0,1N_t$		$9,914*10^3$	0,9915	$9,411*10^7$	2,063	0,4051423
sin199	$n_0= 0,01N_t$		$9,628*10^2$	1,032	$1,825*10^7$	2,338	1,802048
sin200	$n_0= 0,001N_t$		$9,213*10^1$	1,037	$1,9241*10^6$	4,064	1,82272

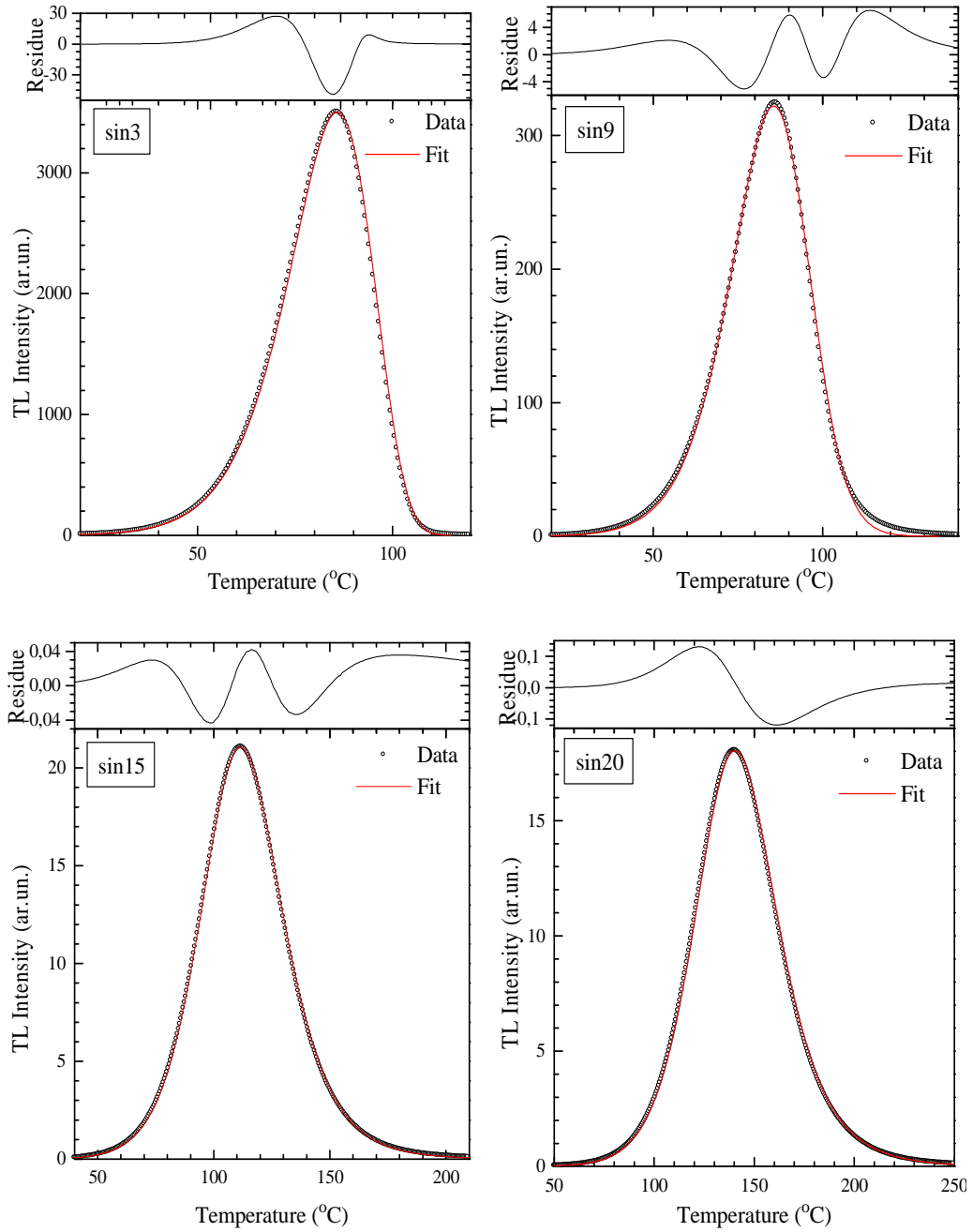


Figure 10. The numerically simulated (open circles) and fitted (red solid line) glow curves of sin3, sin9, sin15 and sin20.

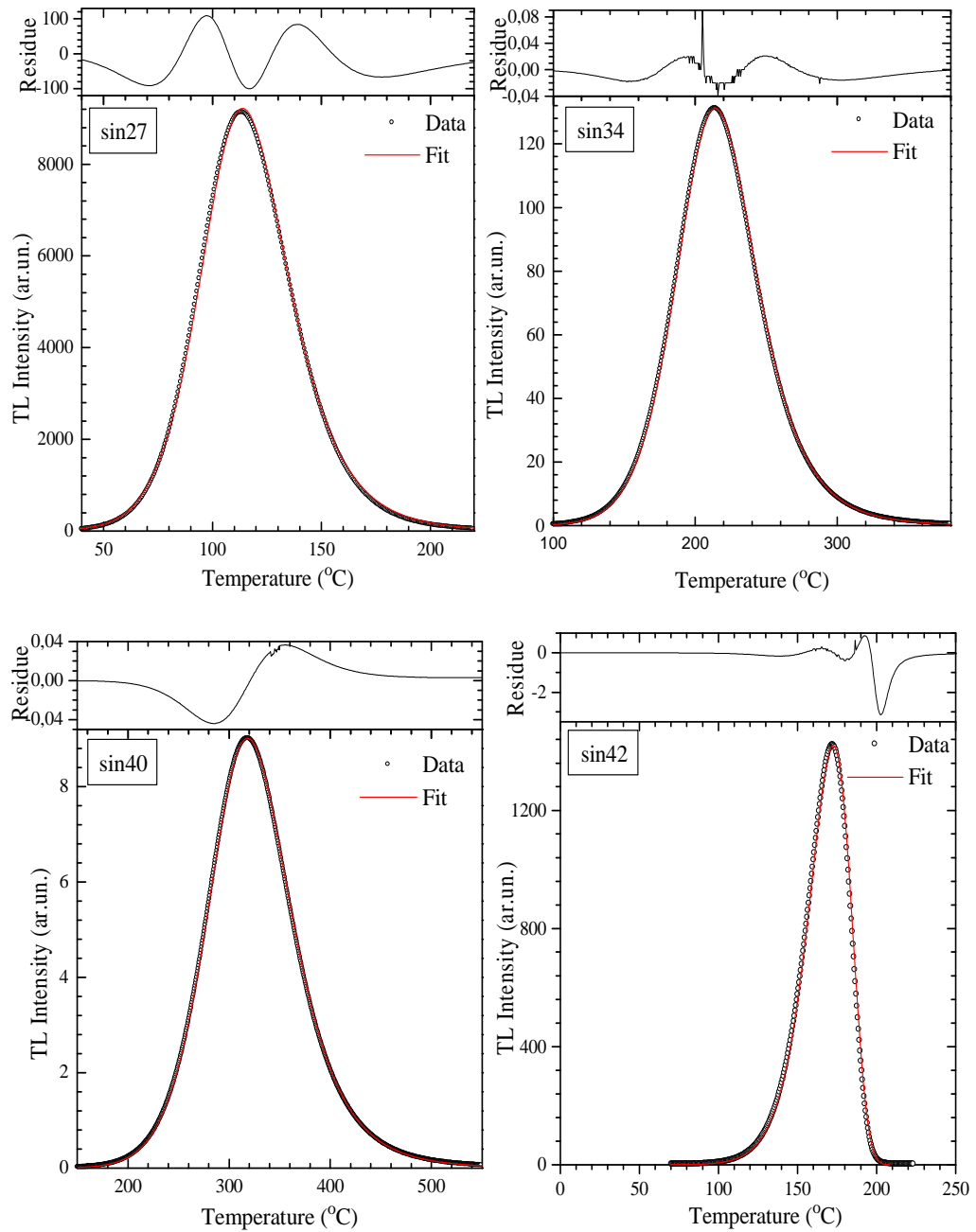


Figure 11. The numerically simulated (open circles) and fitted (red solid line) glow curves of sin27, sin34, sin40 and sin42.

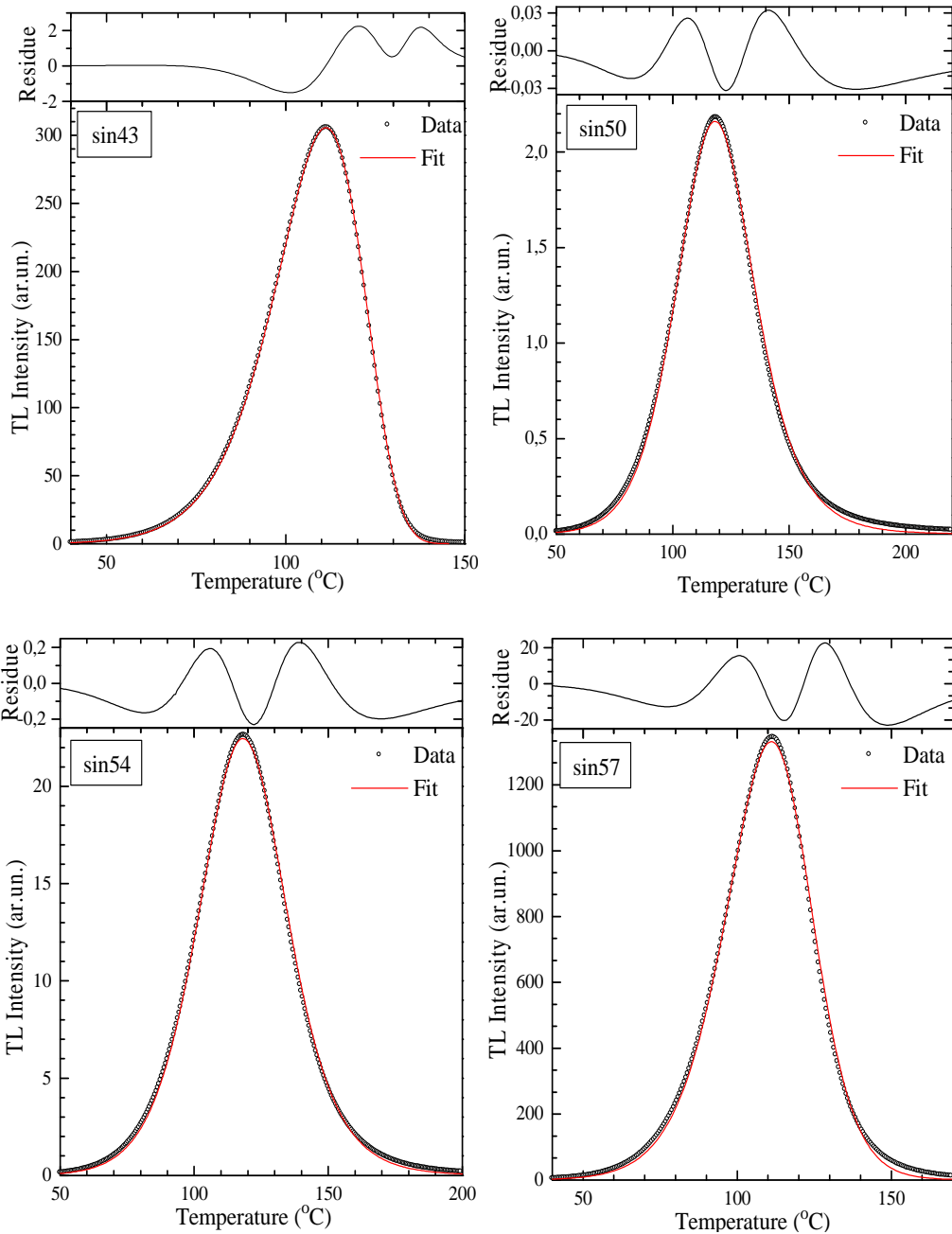


Figure 12. The numerically simulated (open circles) and fitted (red solid line) glow curves of sin43, sin50, sin54 and sin57.

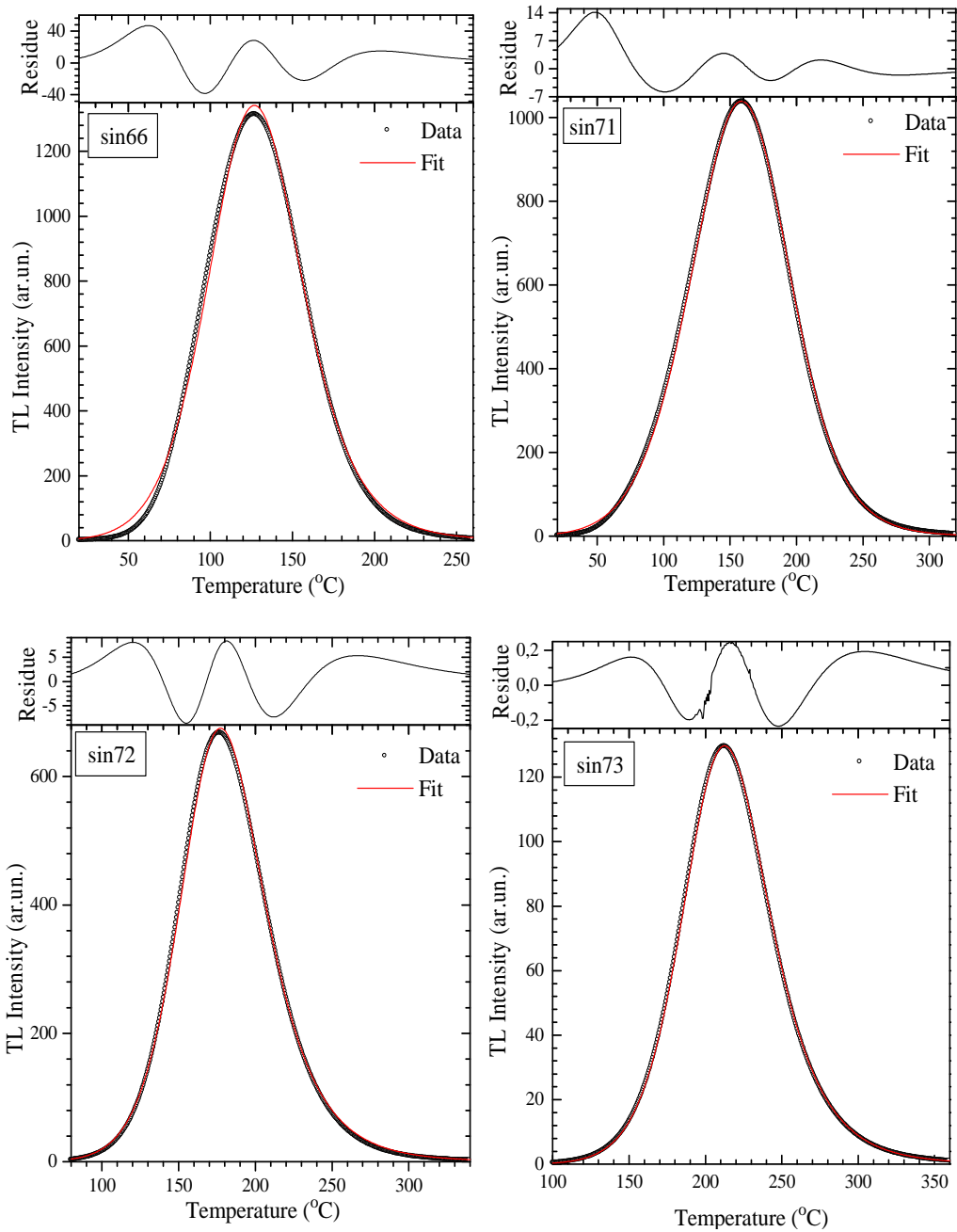


Figure 13. The numerically simulated (open circles) and fitted (red solid line) glow curves of sin66, sin71, sin72 and sin73 .

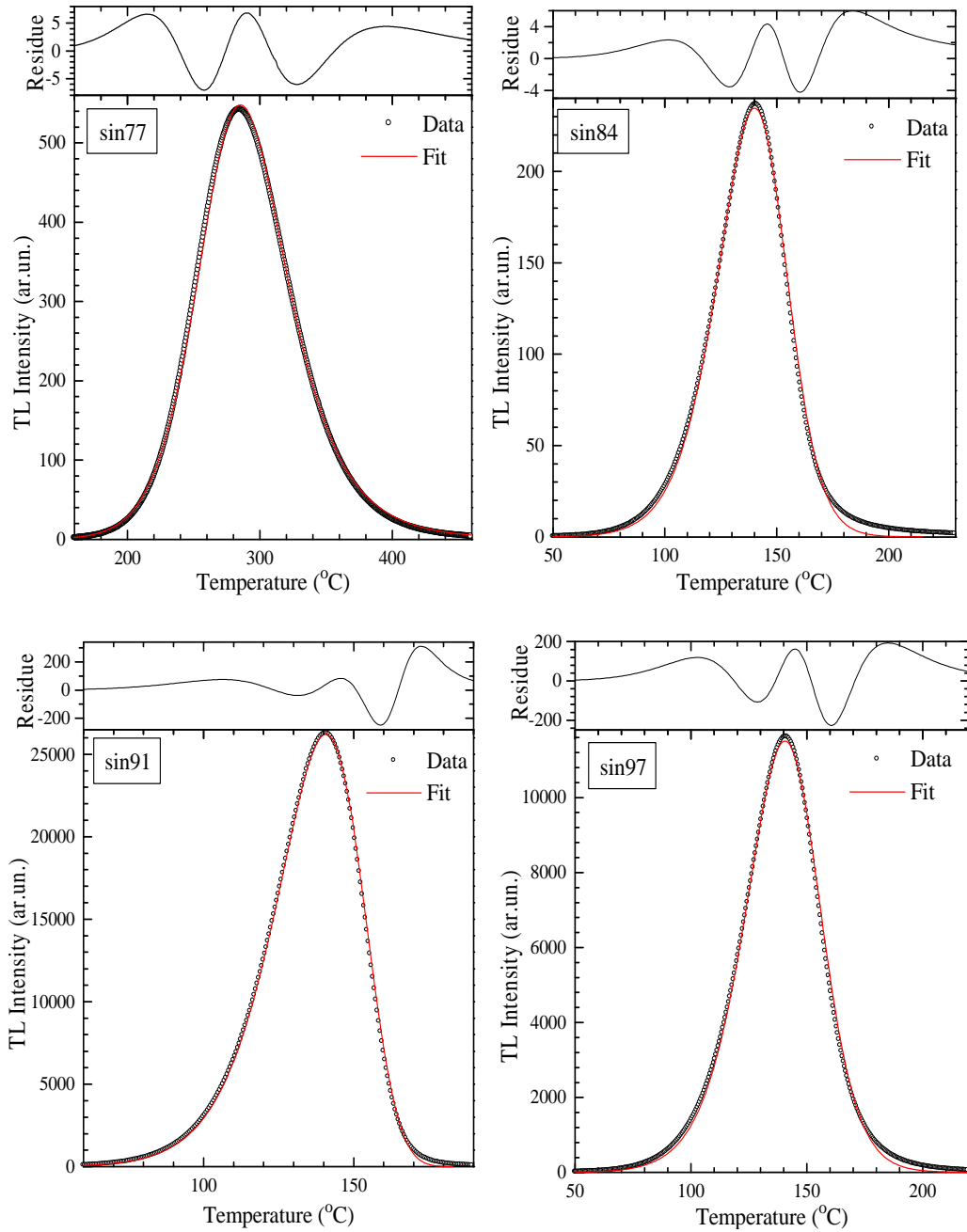


Figure 14. The numerically simulated (open circles) and fitted (red solid line) glow curves of sin77, sin84, sin91 and sin97.

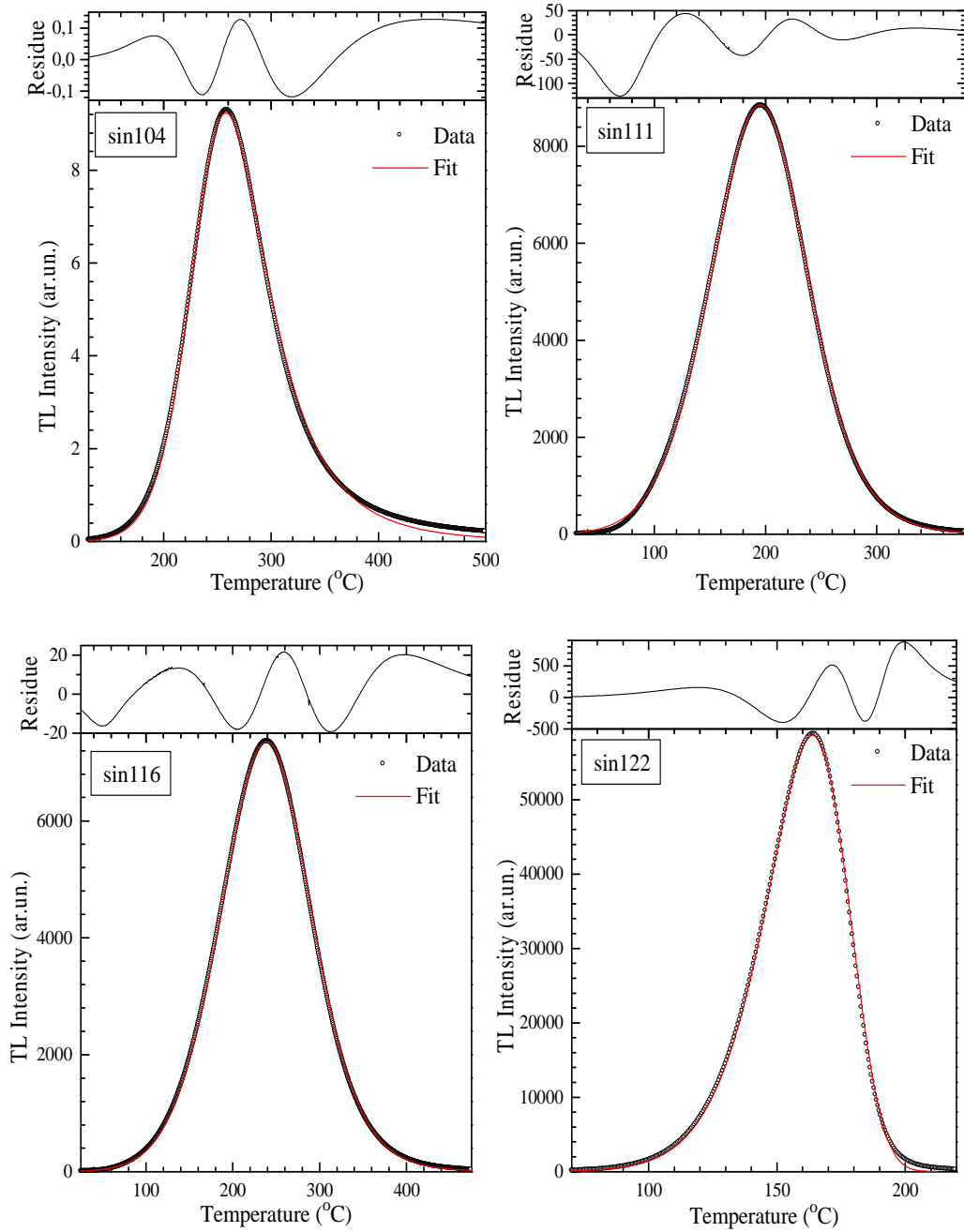


Figure 15. The numerically simulated (open circles) and fitted (red solid line) glow curves of sin104, sin111, sin116 and sin122.

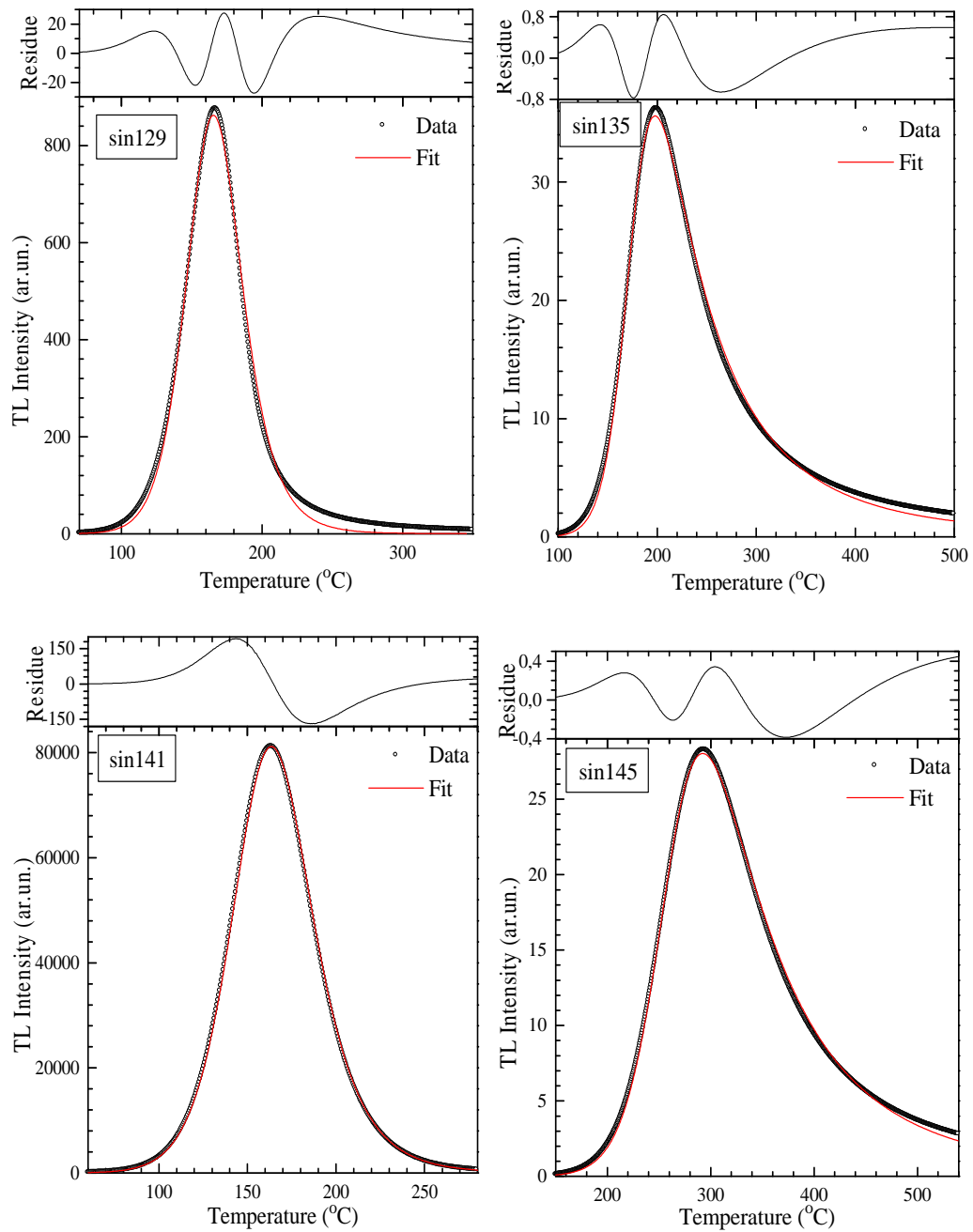


Figure 16. The numerically simulated (open circles) and fitted (red solid line) glow curves of sin129, sin135, sin141 and sin145.

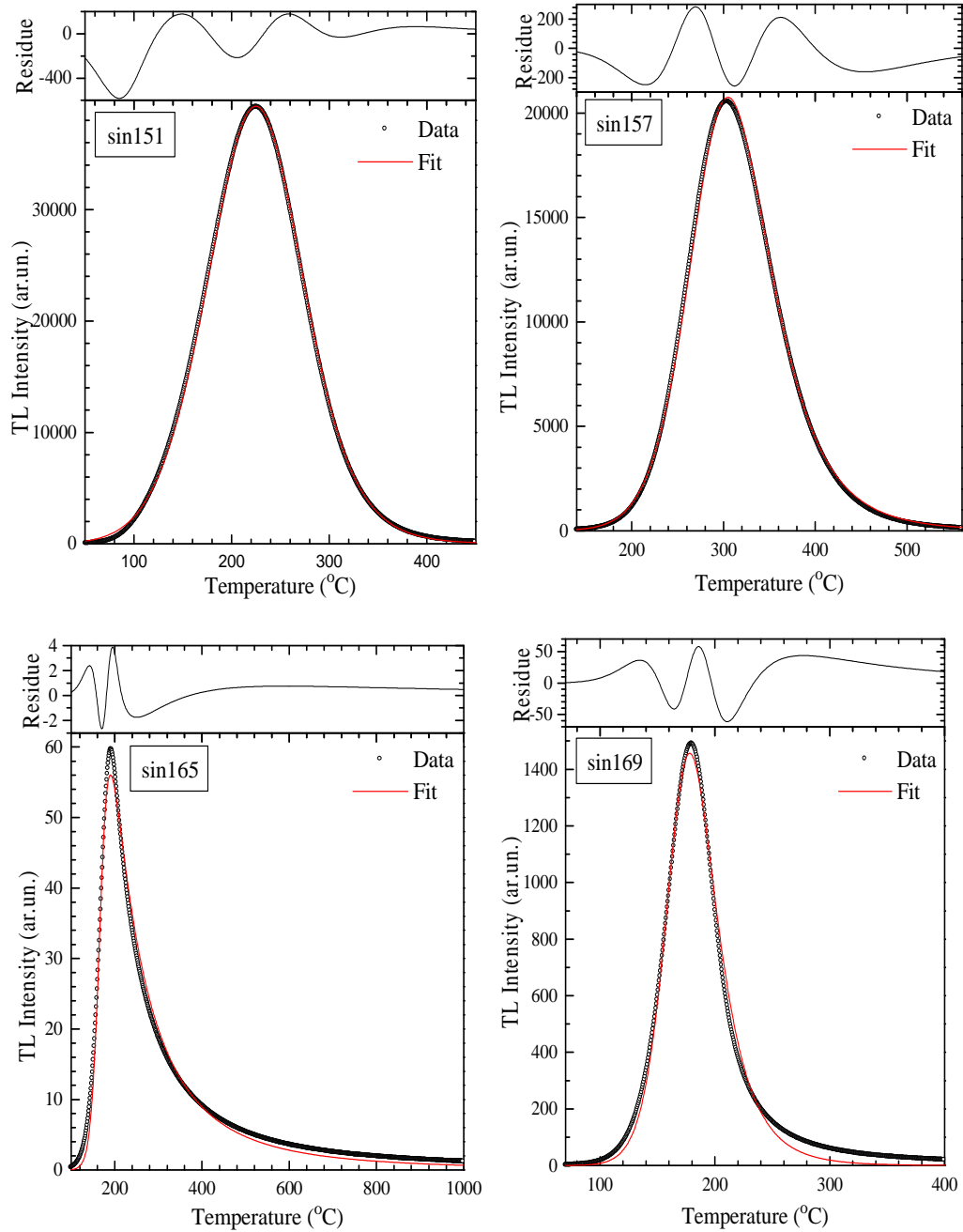


Figure 17. The numerically simulated (open circles) and fitted (red solid line) glow curves of sin151, sin157, sin165 and sin169.

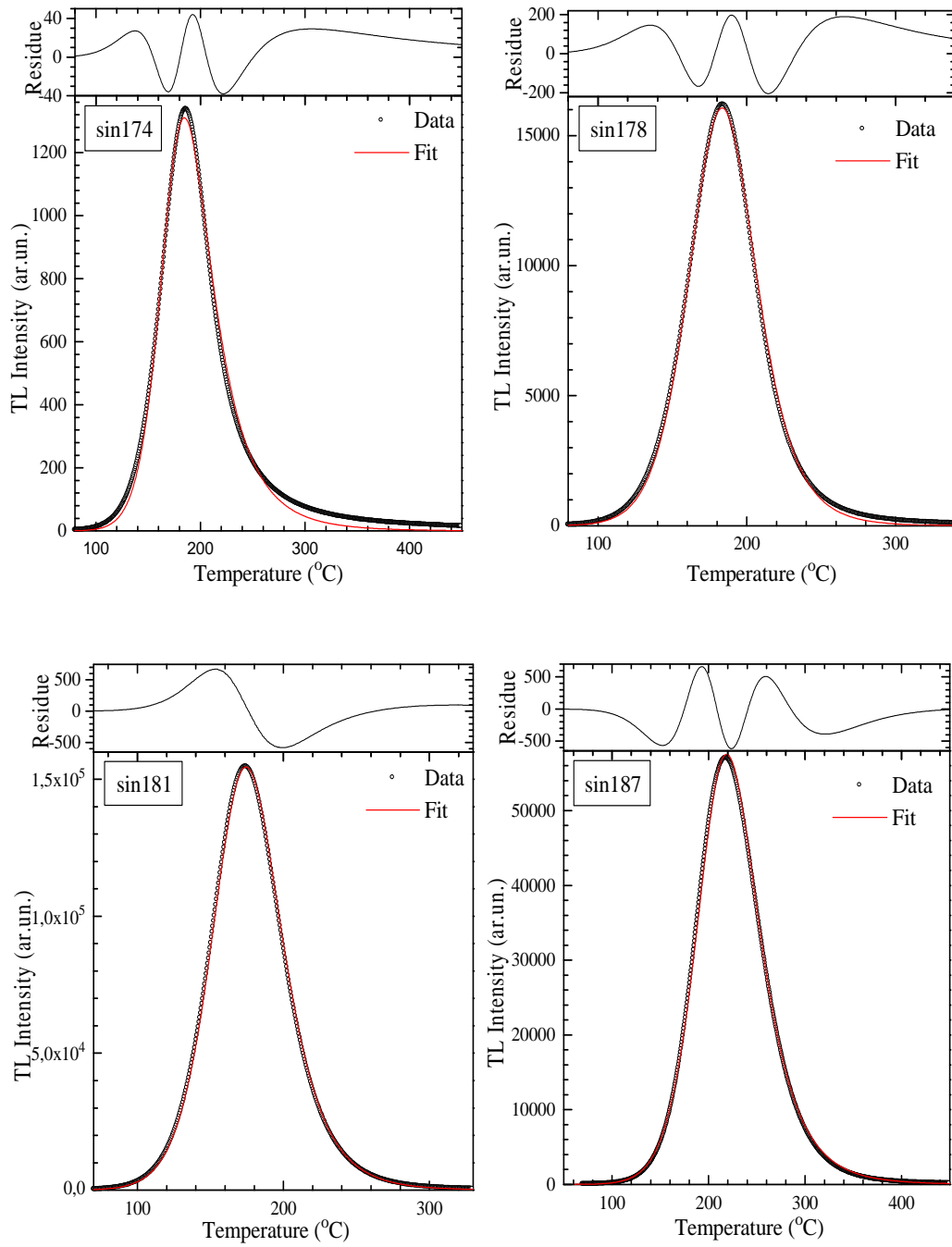


Figure 18. The numerically simulated (open circles) and fitted (red solid line) glow curves of sin174, sin178, sin181 and sin187.

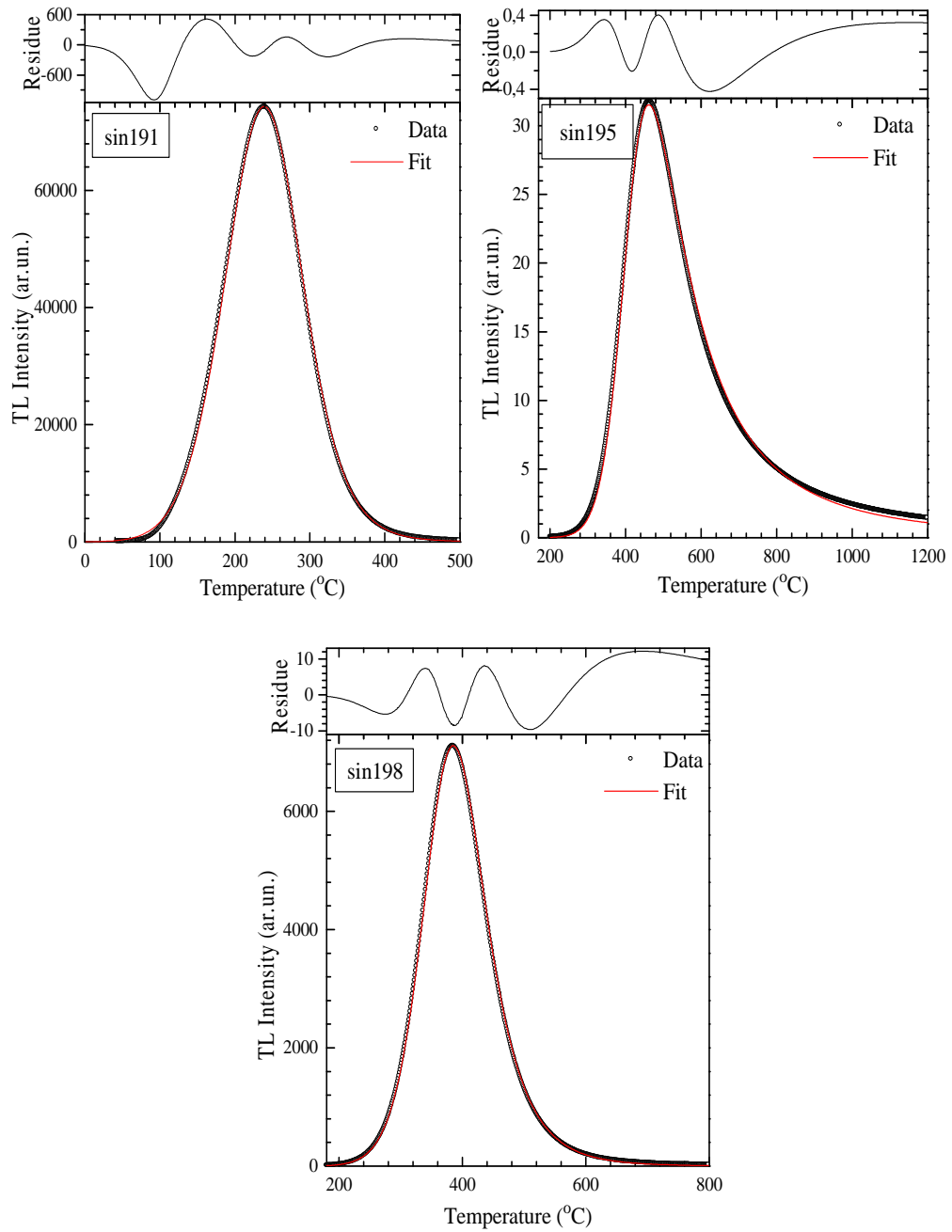


Figure 19. The numerically simulated (open circles) and fitted (red solid line) glow curves of sin191, sin195 and sin198.

CONCLUSION

As mentioned previously, the deconvolution and analysis of the glow curve into its individual glow peaks by computerized curve fitting method has become very popular over the forty years [2, 19]. The computerized glow curve deconvolution (CGCD) is easily performed by available software and it has established that it is not only a powerful technique in the analysis of glow curves but also for studying TL dosimetry (TLD) as well. In dosimetric investigations, it may be necessary to separate the glow curve into its individual glow peaks and finds the values for the glow peak parameters. This can be done by glow curve deconvolution program finding a mathematical model that describes the individual glow peaks. Probably the best deconvolution software program (GLOCANIN) is developed at the Reactor Institute at Delft, The Netherlands [19]. This program has been successfully used in TL&OSL laboratory in our department over a number of years. On the other hand, it is well known that the CGCD method cannot yield the correct trapping parameters in cases where two or more peaks are highly overlapped [38]. Because, the results of curve fitting programs vary strongly for a complex glow curve where includes many closely overlapped glow peaks which have similar intensities. In addition, the values of E_a , s , n_o and b obtained by curve fitting program are highly depending upon the input parameters which were used in the fitting program. It can be mentioned that the values of kinetic parameters are also affected from the different equations, approximations and minimisation procedures that were used in the curve fitting programs. As a consequence, one may wonder whether the results of curve fitting program reflect correct values of trapping parameters of TL materials or not. In the case of experimentally measured glow curves of a real TL material, a difficulty arises in comparing the results of curve fitting programs with the real values of trapping parameters of glow peaks. Because, the true values of these parameters are not known and therefore the inter comparisons of obtained parameters concentrated on the goodness of the fit are meaningless. In addition, anomalous heating and spurious luminescence which are sometimes caused by dosimeter contamination, or light

leakage in the heating chamber, among other causes of measurement artifacts are other problems which are known to affect TL investigations in experimental measurements. Even a minor occurrence of these anomalies distorts the glow curve shape, which is reflected by the numerical values of the very sensitive trapping parameters. This problem is particularly important to obtain kinetic parameters of glow peaks in the solid state investigations. This is a unique problem of TL provided by glow curve deconvolution. However, the input parameters are known in the synthetic glow curves. Therefore, to evaluate the capabilities of the curve fitting programs, it is necessary to obtain synthetic glow peaks by solving the differential equations which describes the charge transport in the TL phenomena by computer simulation and then the numerically obtained glow curves can be analyzed by curve fitting program. The numerical method to analyze TL curves using the rate equations has been studied over forty years [33-34].

In the given study, the synthetic glow curves were firstly numerically obtained by directly solving the differential equations without the use of approximating functions that have no physical meaning after different heating rates and then the inter comparison of input parameters and results of curve fitting program was done. The synthetic glow curves include a single glow peak. Because, as mentioned previously, for well-separated glow peaks, it was observed that the quality of deconvolution is quite satisfactory. However, it has its limitations when the glow peaks are highly overlapped. In the case of simple glow curves, it can be easily analyzed by the CGCD method and the results of fitting can be easily compared to input values, whether it reflects correct values of input parameters or not. In this case, the agreement between the two sets of values is a proof of the adequacy and integrity of the deconvolution program. In contrast, disagreement will imply the existence of anomalies. The fitting program produces a data file with the analysis results, including many parameters such as the number of trapped electrons n_0 (electrons/cm³), the activation energy E (eV), the frequency factor (s (s⁻¹)) and kinetic order b for every peak. Additionally, a plot of residuals, i.e. of the relative differences between measured and fitted values in each channel, FOM values are also included in the data file.

In figures 10-19, some of the selected simulated glow curves after different input parameters (open circles) and fitted glow curves (red solid line) are clearly shown. As seen, the agreement between simulated and fitted glow curves is very

good in most cases. For example, when the input parameters were chosen as very close to the first-order ($A_n \ll A_h$) and second-order ($A_n \approx A_h$) kinetics, the success of the fitting is excellent. Especially, if the number of trapped electrons in electron traps (n_o) is equal or very close to the number of electron traps (N_t), the agreement between simulated and fitted glow curves becomes excellent. On the other hand, if the transition coefficient for electrons in the conduction band becoming trapped (A_n) is greater than the recombination transition coefficient for electrons in the conduction band with holes in centers (A_h), the agreement between numerically simulated and fitted glow curves is decreased at all heating rates. Especially, the success of fit is very bad at the high values of A_n/A_h ratio. Similarly, it was obtained that the success of fitting is influenced by the agreement between input values and fits of results. For example, the agreement between two sets of values is very good near the first-order and second-order kinetics (see tables 1-5). The deviations in the activation energy (E) and frequency factor ($\ln(s)$) are very low and they are in the range from 0% to 10% and 0% to 5%, respectively. It is seen that the values of E obtained by fitting program are always greater than the input parameters up to $A_n = A_h$. However, the agreement between simulated and fitted glow curves is started to disappear when the A_n/A_h ratio is increased above 1 (one). For example, for completely filled traps ($n_o = N_t$) at all $A_n > A_h$, it can be seen that the values of E and s obtained by fitting program are too low when compared with the input parameters of E and s at all heating rates (see tables 1-5). In general, if A_n is greater than A_h , the E and s values obtained by fitting programs are less than the input parameters. The deviations and agreements between the kinetic parameters (n_o , E , s and b) of input values used in the numerical simulated glow curves and fitted results are clearly shown in tables 1-5. The comparisons of fitted parameters and input parameters indicate that the goodness of fit and agreement between input and fitted parameters are highly depend upon the ratio of transition coefficients (A_n/A_h) and occupancies of electron traps by electrons (n_o/N_t), and slightly depend upon the heating rate.

REFERENCES

- [1] S.W.S. McKeever, (1985). “*Thermoluminescence of Solids*”, Cambridge University Press, Cambridge,
- [2] Y.S. Horowitz and D. Yossian, (1995). “Computerized Glow Curve Deconvolution: Application to Thermoluminescence Dosimetry”, *Radiation Protection Dosimetry*, **60(1)**, 1-114,
- [3] R. Chen, S.W.S. McKeever, (1997). “*Theory of Thermoluminescence and Related Phenomena*”, World Scientific, Singapore.
- [4] C. Furetto, Pao-Shan Weng, (1998). “*Operational Thermoluminescence Dosimetry*”, World Scientific, Singapore.
- [5] S. Basun, G. F. Imbusch, D. D. Jia and W. M. Yen, (2003).”The Analysis of Thermoluminescence Glow Curves” *Journal of Luminescence*, **104**, 283-294,
- [6] A.N.Yazıcı, (1996). “*Thermal and optical Characteristics of Radiation Induced Defect Centers in Alkali Halide Crystal*”, PhD Thesis, Gaziantep University.
- [7] Daniels F, Boyd C A, Saunders D F. (1953). “Thermoluminescence as a research tool”, *Science*, **117**, 343.
- [8] F. M. Khan, (2003).”*The Physics of Radiation Therapy*”. Lippincott Williams&Wilkins.
- [9] Y.S. Horowitz (Ed.), (1984). “*Thermoluminescent and Thermoluminescent Dosimetry*”, Vols. 1–3, CRC Press, Boca Raton, FL.
- [10] D.R. Vij, Editor, (1993). “*Thermoluminescent Materials*”, PTR Prentice-Hall, New Jersey .
- [11] S.W.S. McKeever, M.Moscovitch and P.D.Townsend, (1995). “*Thermoluminescence Dosimetry Materials: Properties and Uses*”, Nuclear Technology Publishing, Kent
- [12] V.E.Kafadar, A.Necmeddin Yazıcı and R.Güler Yıldırım, (2009). “Determination of trapping parameters of dosimetric thermoluminescent glow peak of lithium triborate (LiB3O5) activated by aluminum” *Journal of Luminescence*, 129(7), 710-714.
- [13] J.T. Randall and M.H.F. Wilkins, (1945). “Phosphorescence and. Electron Traps: I Study of Trap Distributions,” *Proc. R. Soc. London Ser. A* 184, 366.
- [14] A.J.J. Bos, (2001). “High sensitivity thermoluminescence dosimetry” *Nuclear Instruments & methods in Physics Research Section B: Beam Interactions with Materials and Atoms*, 184(1-2), 3-28.
- [15] C.Furetta, (2003). “*Handbook of Thermoluminescence*”, World Scientific Publishing.
- [16] G. Kitis, J.M. Gomez-Ros and J.W.N. Tuyn, (1998). “Thermoluminescence glow-curve deconvolution functions for first, second and general orders of kinetics”, *Journal of Physics D:Applied Physics*, 31(19), 2636-2641.

- [17] A.J.J.Bos, T.M.Piters, J.M.Gómez Ros, and A.Delgado, (1993). "*GLOCANIN, an Intercomparison of Glow Curve Analysis Computer Programs*", IRI-CIEMAT Report 131-93-005 (IRI, Delft).
- [18] G.F.J. Garlick and A.F.Gibson, (1948). "The electron trap mechanism of luminescence in sulphide and silicate phosphors" *Proc.Phys.Soc.*, 60, 574-590.
- [19] A.J.J. Bos and J.B. Dielhof, (1991). "The Analysis of Thermoluminescent Glow Peaks in CaF₂:Tm (TLD-300)", *Radiat.Prot.Dosim.* 36, 231.
- [20] C.E. May and J.A. Partridge, (1964). "Thermoluminescent kinetics of alpha irradiated alkali halides", *Journal of Chemical Physics*, 40, 1401-1409.
- [21] P.Vasilis, G.Kitis and C.Furetta, (2006). "*Numerical and Practical Exercises in Thermoluminescence*", Springer.
- [22] R. Chen and A.A. Winer, (1970). "Effects of various heating rates on glow-curves", *J.Appl.Phys.* **41**, 5227.
- [23] T.M. Piters and A.J.J. Bos, (1993). "A model for the influence of defect interactions during heating on thermoluminescence in LiF:Mg,Ti (TLD-100)", *J.Phys.D:Appl.Phys.* **26**, 2255.
- [24] R. Chen. (1969). "On the Calculation of the Activation Energies and Frequency Factors from Glow-Curves", *J.Appl.Physics*, **40**, 570.
- [25] L. I. Grossweiner. (1953) . "A note on the analysis of first-order glow curves", *J.Appl.Physics* **24**, 1306.
- [26] A. Halperin and A.A Braner, (1960). "Evaluation of Thermal Activation Energies from Glow Curves", *Phys.Rev.* **117**, 405.
- [27] A.H. Booth, (1954). "Calculation of electron trap depths from thermoluminescence maxima", *Can. J.Chem.* **32**, 214.
- [28] J. Azorin. (1986). "Determination of Thermoluminescence Parameters from Glow Curves: A review", *Nucl.Tracks* **11**, 159.
- [29] 1573.
- [30] N. S. Mohan and R. Chen, (1970). "Numerical Curve Fitting for calculating Glow Parameters", *J.Phys.D:Appl.Phys.*, 3, 243-247.
- [31] D. Shenker and R. Chen, (1972). "Numerical Solution of the Glow Curve Differential Equations", *J.Comp.Phys.*, 10, 272-283.
- [32] H.G. Balian and N.W. Eddy, (1977). "Figure-of-Merit (FOM), an Improved Criterion over the Normalized Chi-Squared Test for Assessing Goodness-of-Fit of Gamma-Ray Spectra Peaks", *Nucl. Instrum.Methods*, 145, 389-395.

- [33] S. K. Misra and N.W.Eddy, (1979). "IFOM, a Formula for Universal Assessment of Goodness-of-Fit of Gamma Ray Spectra", *Nucl.Instrum.Methods*, 166, 537-540.
- [34] A.Necmeddin YAZICI and M.Yakup HACIİBRAHIMOĞLU, (2001). "Determination of the Trapping Parameters of Glow Peaks of CaF₂ :Dy (TLD-200) by Using Computer Glow Curve Deconvolution Method", *Turk J Phys.* 25(3), p.249-255,

